Diet-Related Metabolic Perturbations of Gut Microbial Shikimate Pathway-Tryptamine-tRNA Aminoacylation-Protein Synthesis in Human Health and Disease

International Journal of Tryptophan Research
Volume 12: 1–19

DOI: 10.1177/1178646919834550

Elena L Paley[1,2,3]

[1]Expert BioMed, Inc., Miami Dade, FL, USA. [2]Stop Alzheimers Corp, Miami Dade, FL, USA.
[3]Nova Southeastern University, Fort Lauderdale, FL, USA.

ABSTRACT: Human gut bacterial Na(+)-transporting NADH:ubiquinone reductase (NQR) sequence is associated with Alzheimer disease (AD). Here, Alzheimer disease-associated sequence (ADAS) is further characterized in cultured spore-forming *Clostridium sp*. Tryptophan and NQR substrate ubiquinone have common precursor chorismate in microbial shikimate pathway. Tryptophan-derived tryptamine presents in human diet and gut microbiome. Tryptamine inhibits tryptophanyl-tRNA synthetase (TrpRS) with consequent neurodegeneration in cell and animal models. Tryptophanyl-tRNA synthetase inhibition causes protein biosynthesis impairment similar to that revealed in AD. Tryptamine-induced TrpRS gene-dose reduction is associated with TrpRS protein deficiency and cell death. In animals, tryptamine treatment results in toxicity, weight gain, and prediabetes-related hypoglycemia. Sequence analysis of gut microbiome database reveals 89% to 100% ADAS nucleotide identity in American Indian (Cheyenne and Arapaho [C&A]) Oklahomans, of which ~93% being overweight or obese and 50% self-reporting type 2 diabetes (T2D). Alzheimer disease-associated sequence occurs in 10.8% of C&A vs 1.3% of healthy American population. This observation is of considerable interest because T2D links to AD and obesity. Alzheimer disease-associated sequence prevails in gut microbiome of colorectal cancer, which linked to AD. Metabolomics revealed that tryptamine, chorismate precursor quinate, and chorismate product 4-hydroxybenzoate (ubiquinone precursor) are significantly higher, while tryptophan-containing dipeptides are lower due to tRNA aminoacylation deficiency in C&A compared with non-native Oklahoman who showed no ADAS. Thus, gut microbial tryptamine overproduction correlates with ADAS occurrence. Antibiotic and diet additives induce ADAS and tryptamine. Mitogenic/cytotoxic tryptamine cause microbial and human cell death, gut dysbiosis, and consequent disruption of host-microbe homeostasis. Present analysis of 1246 participants from 17 human gut metagenomics studies revealed ADAS in cell death diseases.

KEYWORDS: human gut metabolomics, database sequence-analysis, shikimate pathway, aminoacyl-tRNA deficiency, dysbiosis, host-microbe interaction, cytotoxicity, tryptophan metabolism, diet, cell death diseases

RECEIVED: August 19, 2018. **ACCEPTED:** February 4, 2019.

TYPE: Original Research

FUNDING: This work was supported by Art Medicus PLLC, Yonkers, NY, USA.

DECLARATION OF CONFLICTING INTERESTS: The author(s) declared no potential conflicts of interest with respect to the research, authorship, and/or publication of this article.

CORRESPONDING AUTHOR: Elena L Paley, Expert BioMed Inc, Stop Alzheimers Corp. 11933 SW 271st TER Homestead, FL 33032 USA. Email: elena_paley@bellsouth.net

Introduction

Gut microbiota has received attention in recent research of Alzheimer disease (AD).[1–3] This study links neurodegeneration and cell death induced by tryptophan (Trp)-derived tryptamine with the presence of gut bacterial Na(+)-transporting NADH:ubiquinone reductase (NQR) sequence associated with AD (ADAS) in different human populations. The tryptamine precursor Trp and an NQR substrate ubiquinone (Q) are shikimate pathway (SP) products synthesized from a common precursor chorismate in human gut. Here, ADAS is further characterized with updated National Center for Biotechnology Information (NCBI) database search. No data on human gut metagenomics and metabolomics are available for AD to date. The results of BLAST (Basic Local Alignment Search Tool) search for high similarity to ADAS in gut metagenomic databases are presented here. A high nucleotide sequence identity to ADAS prompted a discovery of AD link to associated diseases and gut bacteria. Here, a crosstalk between Trp-tryptamine pathway and ADAS analyzed in different gut metagenomics and metabolomics studies.

Our report of 1991 describes the cytotoxicity and formation of tangles of filaments in mammalian kidney cells induced by Trp-decarboxylated metabolites tryptamine and tryptophanol at the concentrations inhibiting enzyme of protein biosynthesis tryptophanyl-tRNA synthetase (TrpRS).[4,5] The assumption was that cells resistant to TrpRS inhibitors competitive to substrate Trp would survive via TrpRS gene (WARS) amplification and increase in TrpRS enzymatic activity. The human pancreatic cancer cells overexpress TrpRS due to duplication/multiplication of chromosome 14, in which WARS is located.[6] In HeLa cells treated with tryptamine, TrpRS had longer half-life than in control cells.[7] The tryptamine-treated neuroblasts recovered growth or transdifferentiated after being transferred to new tryptamine-free culture media.[8] Tryptamine elicited a concentration-dependent mitogenic response.[9] Therefore, tryptamine can induce dose- and cell type-dependent cell death, transdifferentiation, and division. Such combination was observed in about 80% of pancreatic cancer patients having glucose intolerance or frank diabetes,[10] thus joining together the disease of accelerated cell division (cancer) with a cell death disease (diabetes with death of β-cells in Langerhans islets) in the same organ. Moreover, diabetes can be reversed after gastric bypass surgery in morbidly obese patients,[11] probably due to transdifferentiation associated with altered metabolic production by gut microbiota. Neuronal human cell model of tryptamine-induced cell death and formation of neurofibrillary

tangles of filaments (NFT) similar to manifestations in AD brain was discovered (Paley, US Patent 6,221,662; 2001). In our study, tryptamine induces neuronal loss and NFT formation in mouse brain.[12]

We also reported that treatment of human cancer cervical cells HeLa; Chinese hamster SV40-transformed embryonic 631 cells; Djungarian hamster DM15 fibroblasts; Madin-Darby bovine kidney (MDBK) cells; and human neuroblastoma SH-SY5Y cell variants by tryptamine induce a cell density-dependent cytotoxicity.[4,7,12–14] Tryptamine cytotoxicity was shown by other authors on human Jurkat T leukemia cells[15]; HT22 mouse, SK-N-SH human neuronal cell lines, primary cultures of astrocytes from rat brain[16]; and on human monocytic cell line MonoMac6.[17] Tryptamine acute toxicity was demonstrated in mice[18] and rats.[19] In addition, tryptamine is toxic for bacteria, yeast, and plant. Tryptamine ⩽20 μg/mL prevents growth of most cyanobacteria and eukaryotic microalgae. However, most algae recovered growth after being transferred to tryptamine-free culture media, while most cyanobacteria showed no growth recovery.[20] Tryptamine was used in affinity chromatography on agarose hexyl-adenosine-5′-phosphate gel to purify *Escherichia coli* TrpRS.[21] This affirms the specific binding of tryptamine to bacterial TrpRS. Tryptamine at the concentration of 1.6 mM leads to 50% reduction in the initial rate of Trp-dependent [^{32}PPi]-adenosine triphosphate (ATP) exchange reaction catalyzed by *E coli* TrpRS in the presence of 2 mM Trp.[21] Both cyanobacteria and *E coli* present in human gut microbiome. Hence, tryptamine under concentration lower than Trp leads to tryptophanyl-tRNA deficiency with consequent decrease in protein translation in gut bacteria. Tryptamine binds with high affinity to surfaces of pathogenic microorganisms *E coli*, fungus *Candida albicans*, and *Pseudomonas aeruginosa*.[22] Tryptamine stimulates internalization and adherence of staphylococci in human colon adenocarcinoma cell line HT29.[17] Staphylococcal strains produce tryptamine and other biogenic amines (BA), tyramine, and phenethylamine (PEA) through the activity of aromatic amino acid decarboxylase (AAAD) under aerobic and anaerobic conditions.[17] Staphylococci producing tryptamine were isolated from the human gut. The scattered distribution of BA suggests that the corresponding gene(s) was probably acquired by horizontal gene transfer, and that in one given species, not necessarily all members were positive or negative, as shown for *Staphylococcus epidermidis*.[16]

Most yeast strains isolated from cow's milk cheeses are tryptamine producers.[23] Tryptamine affects growth parameters in 16 different wine yeasts.[24] The concentration-dependent tryptamine toxic effect is yeast strain-dependent. Tryptamine influenced differently the growth of yeast strains demonstrating inhibition at 100 to 1000 mg/L or no inhibitory effects or even growth stimulatory effect in some strains. Tryptamine produced by fungus *Penicillium sp*. from marine tunicate *Didemnum sp*., which was collected at a depth of 1-2 m.[25] Tryptamine content can be high in human diet, especially in fermented food reaching 2400 mg/kg in Austrian report of 2017.[5,26] In the study of 1973 conducted in the United States, the highest tryptamine concentration (1.1 mg/g) was detected in Blue cheese.[27]

Tryptophan-auxotroph *Chlamydia pneumoniae* responds to Trp starvation by globally increasing transcription while globally decreasing translation.[28] Similarly, ribosome stalling on Trp codons due to competitive TrpRS inhibition resulted from increased tryptamine/Trp ratio causes globally decreasing translation with a consequent cell death in human organs and in human-associated microbiome.

This study provides evidence for direct link between the presence of ADAS[1] and Trp metabolic aberrations in American Indian C&A population with a high prevalence of obesity and type 2 diabetes (T2D)[29] and in other diseases of cell death and uncontrolled cell division. The C&A participants characterized by a reduced abundance of the anti-inflammatory bacterial genus *Faecalibacterium*, along with a fecal metabolite profile similar to dysbiotic states described for metabolic disorders. American Indians are known to be at elevated risk for metabolic disorders.[29]

Materials and Methods

Metabolomic analysis

An analysis of crude data for human fecal metabolite profiles obtained by liquid chromatography-/gas chromatography-mass spectrometry (LC-MS/GC-MS; Metabolon, http://www.metabolon.com/) was conducted. The values analyzed are for Trp metabolites—tryptamine, indole-3-acetic acid (IAA), indolepropionic acid (IPA), kynurenate (Kyn), skatole, and indole-3-carboxylic acid (ICA); AAA—Trp, tyrosine (Tyr), and phenylalanine (Phe); BA—tyramine and PEA; metabolites of SP; and selected dipeptides and tripeptides. The present metabolomic analysis was conducted following discovery of a high identity to ADAS (87%-100%) in the nucleotide sequences from NCBI databases.[5] Here, a high identity to ADAS was found in the gut microbiome study of American Indian communities, members of the C&A Tribes. The present analysis of metadata from Oklahoma study[29] (C&A and non-native individual [NNI] populations) originates from the BLAST search of the NCBI databases with a usage of ADAS sequence as a nucleotide query. Stool samples were collected in Oklahoma for metabolite profiling from 38 C&A adult individuals and 23 NNI (20 adults, 3 children).[29,30] The research was an interdisciplinary campus-community partnership between the University of Oklahoma and the C&A Tribes.

Statistical analyses

Statistical analyses of ADAS detection were performed with Prism 7.02 software (GraphPad, San Diego, CA). Data were expressed as mean ± SD. The groups were compared using unpaired two-tailed *t*-test. *P*-values less than .05 were considered significant. The abundance profiles of metabolites (tyramine and cysteine) from fecal

metabolomics were compared between the sample groups using the non-parametric Kruskal-Wallis test, in which *P*-value less than .05 indicated a significant difference. The significantly different metabolites were visualized in box-plot. The data showing outliner effects (major outliers) removed from some evaluations. The outlier is an extreme value in a set of data, which is much higher or lower than the other numbers. In this study, the examples of minor and major outliners are shown in Figure 1 for tryptamine. It was determined on a case-by-case basis what the effect of the outliers was (Figure 1A) and from there, it was decided whether we want to remove or keep the outlier values.

Here, for some metabolites, a T2D C&A subgroup was used for comparison with NNI, which contains no T2D. The current statistical analysis of the metabolites presented here was conducted using unpaired two-tailed *P*-value parametric (Gaussian distribution) linear regression "do not assume equal" SD *t*-test with Welch correction (Welch test) of the GraphPad Prism 7.04 software. The data between NNI and C&A were considered significantly different at *P*-value less than .05.

Tryptamine cytotoxicity

A human cervical carcinoma cell line HeLa; SV40-transformed embryonic Chinese hamster 631 cells; and their tryptamine-treated sublines were cultivated as a monolayer in RPMI-1640 medium (Trp at 5 mg/mL) under 5% CO_2 at 37°C in plastic flasks (Nunc). The 10% fetal calf serum (FCS), 1 mM glutamine, and antibiotics (100 U/mL penicillin, 100 mg/mL streptomycin, and 0.3 mg/mL amphotericin B) were added to the medium. Sublines surviving tryptamine were selected through stepwise raise in tryptamine concentrations (25, 50, 100, 150, 200, and 250 μg/mL). Note that the possible variations in tryptamine cytotoxic doses could be due to uncontrolled Trp concentrations in FCS used for cell cultivation. The level of free Trp in the medium can be increased by proteolytic enzyme trypsin depending on the cell trypsinization protocol. In addition, the tryptamine cytotoxicity is cell-density dependent. Cell viability was examined by Trypan blue dye exclusion. Cells were plated at 1.8×10^5 per 50 mm plastic Petri dishes containing 4.5 mL of medium, with or without various tryptamine concentrations, and incubated at 37°C under 5% CO_2 for 4 days. The non-adherent presumably non-viable cells were washed off, while the adherent cells were trypsinized and suspended in the fresh medium with Trypan blue. The viable cells were counted in a hemocytometer for each tryptamine concentration.

DNA dot-blot hybridization of WARS gene

The slot blot analysis was performed with DNA from control and tryptamine-treated HeLa and 631 sublines as described.[32] The 2×10^5 cells were loaded into each slot. DNA from cell lysates was denatured in saturated NaI solution at 90°C, immobilized onto nitrocellulose filters and hybridized with a ^{32}P-labeled human TrpRS cDNA probe. The cDNA clones 5 and 9 specific to human TrpRS were used for hybridization.

Immunoprecipitation of steady-state [^{35}S]-labeled TrpRS

For metabolic labeling, the control or tryptamine-treated HeLa cells were plated as for cytotoxicity assay. Following 5 days, the cells were starved in methionine-free Dulbecco's modified Eagle medium (DMEM) with the addition of 10% dialyzed FCS for 2.5 h. The cells were then steady state labeled for 17 hours in methionine-free DMEM with 22 μCi/mL [^{35}S] methionine (3 mL/plate; specific activity 1000 Ci/mmol; Amersham Corp.) and 10% dialyzed FCS. The post-mitochondrial cell extracts were prepared after labeling. The labeled cells were washed twice with ice-cold phosphate-buffered saline (PBS) and then removed from plates with a plastic cell scraper (Costar). Cell extraction was done with 0.5 mL of ice-cold PBS and 5 mM phenylmethylsulfonyl fluoride (PMSF) in a glass homogenizer using 40 strokes of a Teflon pestle. The extracts spun for 15 minutes at 14 000 r/min (Eppendorf centrifuge 5415C) at 4°C. Approximately equal amounts of trichloroacetic acid (TCA)-insoluble radioactive post-mitochondrial supernatants (each sample contained 1.4×10^6 cpm in 0.7 mL) were pretreated with 50 μL of 10% protein A-insoluble *Staphylococcus aureus* suspension.[4] Supernatants were incubated with polyclonal rabbit antiserum to bovine TrpRS or with control non-immune rabbit serum for 1 hour at room temperature. Thereafter, the immune complexes were precipitated by the addition of *S aureus* suspension for 30 minutes at room temperature. The pallets were washed once as above and twice with buffer containing 10 mM Tris-HCl, pH 8.6, 150 mM NaCl, 1% sodium deoxycholate, 1% Triton X-100, 0.1% sodium dodecyl sulfate (SDS), and 1 mM PMSF; once with 10 mM Tris-HCl, pH 7.5, 0.1% SDS, and eluted by boiling with SDS sample buffer for 5 minutes. The [^{35}S]-labeled proteins were separated by 12.5% sodium dodecyl sulfate polyacrylamide gel electrophoresis (SDS-PAGE) and visualized using Amplify (Amersham Corp.). The dried gel was exposed to AGFA film at −80°C.

Immunoblotting of TrpRS from human neoblastic SH-SY5Ycells

Cell treatment for detergent-soluble cell extracts was performed with 20 μg/mL of tryptamine for 1 month and for total extracts with 40 μg/mL for 4 days followed by treatment with 20 μg/mL for 2 days. For SDS extraction, the control and tryptamine-treated epithelial-like cells were washed with PBS, solubilized in situ in buffer containing 2% SDS, 100 mM dithiothreitol (DTT), 50 mM Tris-HCl, and pH 6.8 (100 μL of buffer per 5 cm plate), collected, and boiled for 5 minutes. For Triton extraction, the epithelial-like cells were lysed in 0.1 M HEPES; pH 6.9; 0.5% Triton X-100; 1 mM $MgCl_2$; 0.1 mM EDTA; 2

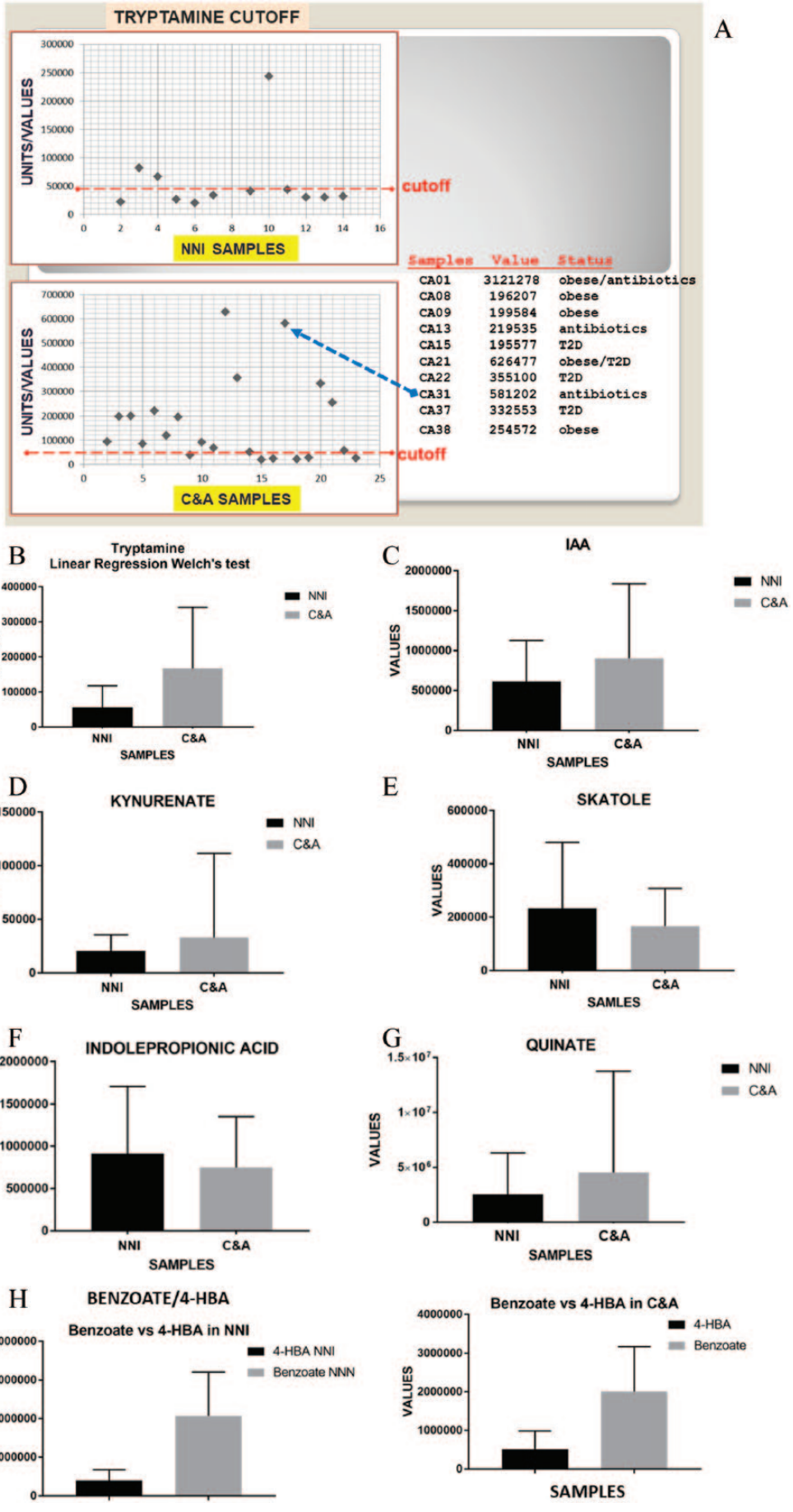

(Figure 1. Continued)

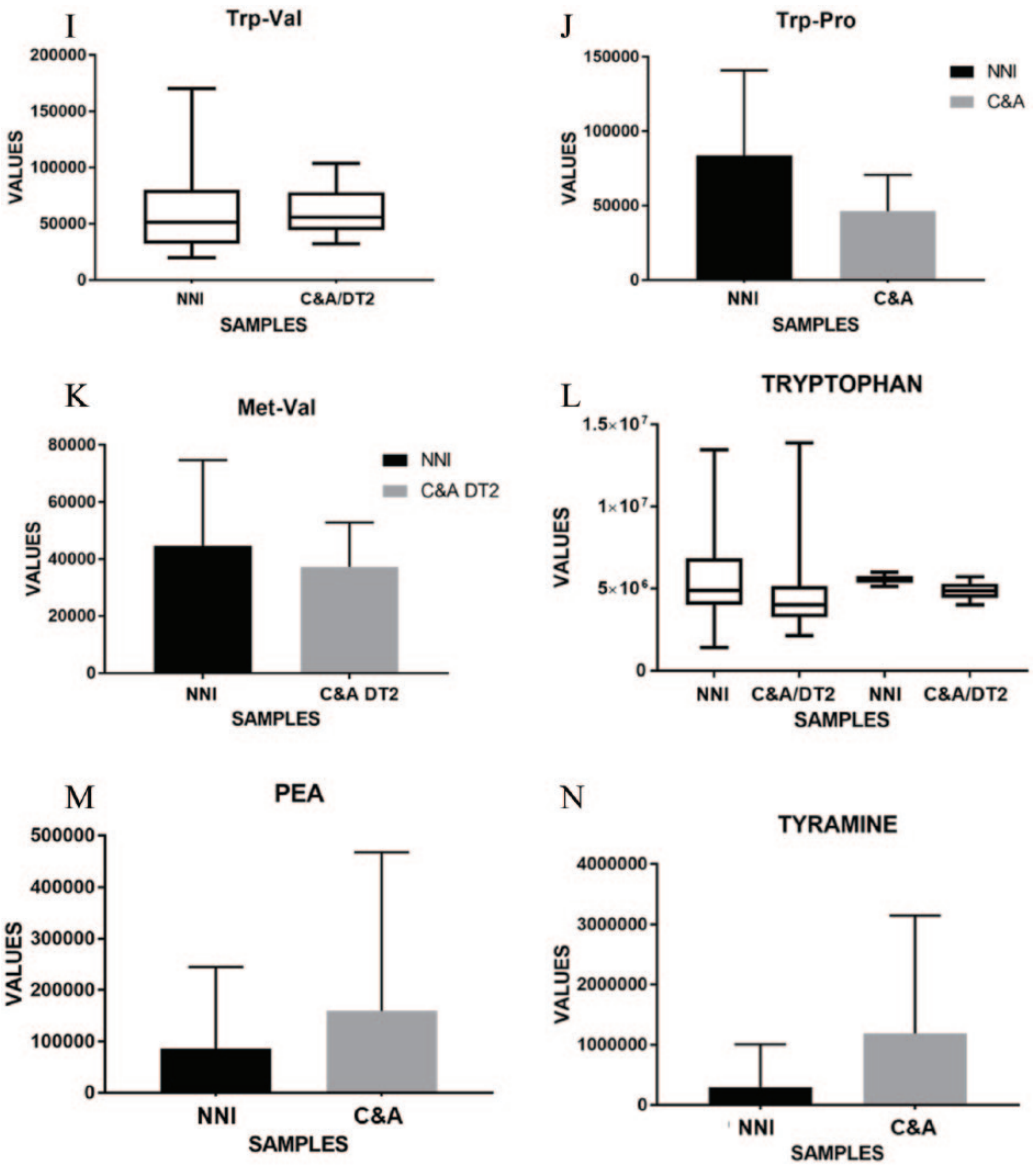

Figure 1. Comparative meta-analysis of crude data for selected metabolites in stool samples of Native American Indian (C&A) and non-native individual (NNI) participants. Figures depicting metabolites show significant differences ($P < .05$) between C&A and NNI populations. Raw metabolite data are provided in the earlier reported Supplemental Table S4.[29] Here, microbiome gut metabolite comparison (Welch test) between C&A and NNI participants is shown as mean ± standard error of the mean (SEM). (A) Using Microsoft Excel software, the tryptamine values were depicted as a scatter chart with determined cut-off line. The table shows tryptamine values above the cut-off level and characteristic values for C&A (CA) individuals. The tryptamine cut-off value of 44 000 units was determined in the graphic of Microsoft Excel software. The major outliers (highest values) are not included in the tryptamine cut-off graphic since the highest values are not directly comparable in the same graphic with essentially smaller values. Meta-analysis of Trp- and Met-containing dipeptides includes the crude data for C&A T2D subgroup. For statistical analyses and data display, any missing values were assumed to be below the limits of detection. The current analysis was restricted to the selected tryptamine pathway-related compounds. The statistical analysis of metabolites was conducted using unpaired two-tailed *P*-value parametric (Gaussian distribution) linear regression "do not assume equal" SD *t*-test with Welch correction (Welch test) of the GraphPad Prism 7.04 software. The original quantitative abundance non-targeted profiles for a total of 535 fecal metabolites were obtained from Metabolon, Inc. Compounds were identified by automated comparison to reference chemical library entries with subsequent visual inspection for quality control as previously described.[31] Human fecal metabolite profiles were obtained by LC-MS/GC-MS. Peaks were quantified using area under the curve. Values in the vertical axis (Y axis) of graphics correspond to peak areas. Welch test (*P*-values and significance*): (B) tryptamine (**$P = .001$); (C) IAA (*$P = .02$); (D) kynurenate (****$P = .0001$); (E) skatole (*$P = .048$); (F) IPA ($P = .14$, ns); (G) quinate (****$P < .0001$); (H) benzoate/4-HBA (****$P < .0001$ for NNI and C&A); (I): Trp-Val (***$P = .0008$); (J) Trp-Pro (***$P = .0002$); (K) Met-Val (*$P = .016$); (L) tryptophan ($P = .4483$, NNI/C&A = 1.14); (M) PEA (*$P = .0152$); and (N) tyramine (****$P < .0001$).

mM EGTA; 1 mM DTT; 1 mM PMSF; 0.4 mg/mL aprotinin; 0.1 mg/mL antipain, leupeptin, pepstatin, and hemastatin; 0.1 μM okadaic acid, 10 mM sodium orthovanadate; and 50 mM sodium fluoride in situ (1 mL of buffer per 8 cm plate) for 20 minutes at room temperature. The equal amounts of proteins (80 μg/lane) of the epithelial-enriched extracts from control

Table 1. Occurrence of nucleotide sequence ADAS in C&A, Oklahoma, Texas (TX), and Missouri (MO) populations of the United States.

DATA	HEALTHY CONTROL, TX/MO (DBGAP)	C&A TRIBES
Participants, N	300	37
Identity to ADAS (89%), N	4	2
Identity to ADAS (100%), N	0	2
Identity to ADAS (89% + 100%), N	4	4
ADAS in population (89%-100%)	1.3	10.8
% obesity in population	0	93
% diabetes (T2D) in population	0	50

Abbreviations: ADAS, Alzheimer disease-associated sequence; C&A, Cheyenne and Arapaho; dbGaP, database of Genotypes and Phenotypes; N, number of individuals; T2D, type 2 diabetes.
Here, 89%-100% nucleotide identity corresponds to 97%-100% amino acid identity.

and tryptamine-treated cells were separated by SDS-PAGE. The blots were incubated with monoclonal antibodies (mAb) 6C10 to TrpRS,[33] washed, incubated with anti-mouse IgG conjugated with horseradish peroxidase, and developed with enhanced chemiluminescence (ECL).

Immunostaining of cerebral blood vessels in AD brain with mAb to TrpRS

The histological AD brain sections were treated and immunostained as described[8,14,33] with anti-TrpRS mAb 9D7 characterized with epitope-mapping.[33]

Treatment of mice: glucose and weight detection, and positron emission tomography

Male mice (8 weeks of age, body weight = 23-26 g) were purchased from the Charles River Laboratories (Wilmington, MA). The mice treatment is described in details elsewhere.[11]

Results and Discussion

Alzheimer disease-associated sequence in human gut

BLAST search for the sequence identity to ADAS[1] was performed in the most recently updated NCBI databases. The four C&A participants (10.8%) with obesity or T2D or obesity/T2D show high nucleotide sequence (kilobase pairs [kbp]) identity to ADAS with 100% identity (~40 and 60 kbp, two individuals) and 89% identity (~40 and ~140 kbp, two individuals) in whole-genome shotgun contigs (wgs) of human gut metagenome. Meta-analysis reveals that obesity and diabetes significantly and independently increase the risk for AD.[34] No ADAS was revealed in the gut metagenome of the control NNI group from Oklahoma. Alzheimer disease-associated sequence presents at 100% nucleotide identity in six individuals possessing near identical ADAS+ fragments (sequence contigs): two C&A, two morbidly obese (Denmark), one control of Washington, DC study, and one patient with ankylosing spondylitis (AS) from China of the entire NCBI database collection (Table 1; Supplemental Table S1). The C&A ADAS+ 60 kbp sequence contig used as a search query reveals a seventh individual possessing fecal DNA with 100% nucleotide identity to ADAS in control healthy subject of China colorectal cancer (CRC) study.[35] Nucleotide sequence of 89% identity to ADAS is more frequent and presents in ~60 individuals with ADAS+ contigs of 99% to 100% identity to each other. Metabolomic profiling is available for three of four C&A individuals with a high identity to ADAS.

The C&A population were compared with the control healthy population in terms of ADAS identity. The four stool samples with 87% nucleotide identity (equal to 97% amino acid identity) to ADAS were found in NCBI dataset of 300 men and women of 18 to 40 years of age from the control healthy population of Houston, TX and St. Louis, MO (Table 1). This population-based control set (database of Genotypes and Phenotypes [dbGaP] study) of the Human Microbiome Project (HMP) addresses whether individuals share a core microbiome. It involves microbiota found in five anatomical sites: the oral cavity, skin, nasal cavity, gastrointestinal tract, and vagina. A high identity to ADAS was found only in stool samples of dbGaP dataset (embargo release February 8, 2018). Therefore, the 1.3% of the healthy US population possesses gut bacterial sequence of 97% amino acid identity to ADAS (Table 1).

Meta-analysis of tryptamine-related human fecal metabolites from NNI and C&A

Most patients with T2D are obese, and the global epidemic of obesity largely explains the dramatic increase in the incidence and prevalence of T2D over the past 20 years. Currently, over one-third (34%) of US adults are obese and over 11% of people aged ⩾20 years have diabetes. Nevertheless, a prevalence of obesity and T2D in C&A is significantly higher than in the general US population. Here, metabolites of C&A individuals with a high proportion of overweight/obese (~93%), obese (~73%), and T2D (~50%) are compared with NNI with 10% of obese, 23% of overweight, and no T2D.[29] The 13 of 41 C&A participants (31%) in metabolomics used unknown antibiotics. I analyzed the crude metadata from Oklahoma study using Welch test for the following: Trp metabolites tryptamine, IAA, Kyn, skatole, IPA, and ICA; AAA Trp, Phe, and Tyr; SP metabolites; BA tyramine and PEA; and di- and tripeptides (Figure 1; Table 2). Table 2 includes the statistical analysis of 20 metabolic compounds. The statistically significant differences between the levels of C&A and NNI fecal metabolites indicate that ADAS occurrence in C&A population correlates

Table 2. Linear regression statistical analyses of mean differences in metabolites of C&A vs NNI in Welch test.

METABOLITE	SIGNIFICANTLY DIFFERENT*	C&A VS NNI MEAN, FOLD
Benzoate/4-HBA	Yes, two-tailed	–1.31
Tryptamine	Yes, two-tailed	+3
IAA	Yes, one-tailed	+1.47
Kynurenate	Yes, one-tailed	+1.65
Skatole	Yes, one-tailed	–1.4
4-HBA	Yes, two-tailed	+1.29
Quinate	Yes, one-tailed	+1.77
Trp-Pro	Yes, two-tailed	–1.8
Trp-Val	Yes, one-tailed	–1.1
Trp	Yes, two-tailed	–1.1
Tyramine	Yes, two-tailed	+4
PEA	Yes, two-tailed	+1.86
Tyrosine	Yes, one-tailed	–1.23
Phenylalanine	Yes, two-tailed	–1.2
Indolepropionate	Yes, two-tailed	–1.23
3-HBA	Yes, one-tailed	–1.04
Leu-Leu-Leu	Yes, one-tailed	+2
Leu-Gly	Yes, one-tailed	+ 1.3
Met-Val	Yes, one-tailed	–1.2
ICA[a]		+1.81

Abbreviations: C&A, Cheyenne and Arapaho Tribes; IAA, indole-3-acetic acid; ICA, indole-3-carboxylic acid; NNI, non-native individuals; PEA, phenethylamine; Trp, tryptophan; 4-HBA, 4-hydroxybenzoate.
[a]ICA detected in 17.4% of NNI and 31.6% of C&A.
*$P < .05$ indicated a significant difference.

with perturbations in tryptamine-related pathways, which may underlay the tryptamine-induced neurodegeneration and cell death in human. Significantly higher tyramine and cysteine in C&A than in NNI estimated here correlate with those reported earlier using different tests (non-parametric Kruskal-Wallis test). Statistical analyses of metabolites are presented here for the first time (Table 2).

Shikimate pathway: 4-hydroxybenzoate, 3-hydroxybenzoate, benzoate, and quinate

The 3-hydroxybenzoate (3-HBA) and 4-hydroxybenzoate (4-HBA) were detected in stool samples of NNI and C&A. Both 3-HBA and 4-HBA are products of chorismate in SP, in which 4-HBA is a Q precursor. Here, the 4-HBA values are significantly higher (1.29-fold) in C&A compared with NNI, while 3-HBA values show small or no difference between the two populations. The 4-HBA synthesized directly from chorismate by the chorismate pyruvate-lyase reaction in bacteria, or from L-tyrosine, similar to higher eukaryotes. Statistically significant mean difference ($P < .0001$) in benzoate/4-HBA ratio (Figure 1; Table 2) was found between NNI (~5-fold) and C&A (~3.8-fold). In *Streptomyces sp.*, benzoate forms directly from shikimate, a precursor for chorismate. Benzoate is widely used by the food industry to prevent spoilage and to inhibit the growth of pathogenic micro-organisms.[36] Sodium benzoate therapy improved symptomatology of patients with schizophrenia.[37] Zinc benzoate, which is commonly used in food and food additives, inhibits monoamine oxidase A (MAO-A) activity.[38] The secondary metabolite of SP quinate is 1.77-fold higher in C&A compared with NNI. Quinate and IAA were found to be correlated with taxa Actinobacteria Atopobium associated with CRC by case-control status.[39] Metabolic crosstalk between the catabolic quinate/SP and the biosynthetic SP produces chorismate. Chorismate is a starting metabolite of branched pathways leading to biosynthesis of AAA and Q. Additional data related to Q are included in Supplemental File 1.

Aromatic amino acid (AAA) and aromatic amino acid/biogenic amines ratio

Tryptophan values (23 NNI and 35 C&A) showed statistically significant lower levels in C&A compared with NNI (–1.1x) in the estimations of Trp/tryptamine ratio (Table 2). Statistically significant difference was found in Trp/tryptamine ratio between NNI and C&A populations. The total Trp levels are significantly higher than tryptamine values in NNI (~100-fold) and C&A (30-fold). The maximal ratio for free Trp/total Trp is ⩽0.005 in human breast milk.[40] Based on this recently reported ratio, the tryptamine mean values are higher than free Trp values in C&A population under the assumption that Trp total/Trp free ratio is 200. The free Trp/tryptamine ratio in C&A population is potentially toxic and sufficient to inhibit TrpRS considering the tryptamine Ki/Trp Km ratio (6-fold) for mammalian TrpRS.[4] The three individuals with a high identity to ADAS express high, medium, and low Trp. A low Trp is detected in obese/T2D individual. The lower trends revealed for other AAA—Tyr (–1.23-fold) and Phe (–1.2-fold) in C&A vs NNI (Table 2). Significant difference in Tyr/tyramine is 36-fold for NNI ($P < .0001$) and 7.4-fold for C&A ($P < .0001$). Significant difference ($P < .0001$) in Phe/PEA is 231-fold for NNI and ~100-fold for C&A.

Biogenic amines: tryptamine, tyramine, and phenethylamine

Present meta-analysis (Figure 1; Table 2) reveals significantly higher (3-fold) tryptamine in C&A participants compared with NNI. Apparently, the determination of tryptamine in human stool samples is the case of tests with continuous results obtained in different studies (Supplemental Figure S1 in this

study[29,41]). Therefore, the most appropriate test cut-off value can be determined. For determining the cut-off value, we need to know the pretest probability of the disease of interest. This means that even for a certain diagnostic test, the cut-off value is not universal and should be determined for each method and for each disease condition. Mostly based on receiver operating characteristic (ROC) curve analysis, there are various methods to determine the test cut-off value.[42] The most common criteria are the point on ROC curve where the sensitivity and specificity of the test are equal. In the present analysis of MS metabolomics, the majority of the control group NNI (64%) and minority of C&A participants (26%) showed values less than 44 000 units. Here, the proposed cut-off value of 44 000 units derived from the quantitative abundance profiles for fecal metabolites is higher in places where the metabolic disease is less prevalent.

The major outliers (highest values) are not included in Figure 1 (tryptamine cut-off in Microsoft Excel software) because the highest values are not directly comparable in the same graphic with essentially smaller values. In three individuals with a high identity to ADAS, the tryptamine values are above the cut-off level. The three individuals with a high and highest tryptamine used antibiotics. Some participants who used antibiotics showed a low tryptamine. We reported a sensitivity of ADAS$^+$ bacteria to a particular antibiotic.[1] Tryptamine, tyramine, and PEA can be produced in C&A gut micro-organisms via AAAD encoded by a single gene[16] because values are higher for tyramine (4-fold) and PEA (1.86-fold) in C&A compared with NNI (Table 2; Figure 1). Obese C&A individual using antibiotics showed a high tyramine, PEA, and ADAS.

Indole-3-acetic acid

Indole-3-acetic acid is a product of tryptamine degradation catalyzed by MAOs. Even though scattering of two populations (23 NNI and 34 C&A) is in some ways similar, the IAA is at a higher trend (1.47-fold) in C&A compared with NNI. In three individuals with a high identity to ADAS, the IAA values range within NNI values with a lowest value for C&A obese/T2D individual. Urinary IAA is significantly higher (~2-fold) in autistic children (30 children) compared with 30 matched controls (age range = 2-7).[43]

Kynurenate

Significantly higher Kyn (1.65-fold) was detected in 25 C&A individuals (66%) compared with 19 NNI (82%). Kynurenate values for two individuals with a high identity to ADAS are available: one is high and another is low. A highest Kyn value was detected in obese/T2D individual (+antibiotics). Significantly higher tryptophan 2,3-dioxygenase (TDO; 4.5-fold, $P < .0001$) and indoleamine 2,3-dioxygenase (IDO) 1 immunoreactivity (2.9-fold, $P < .0001$) were observed in the hippocampus of AD patients.[44] TDO and IDO catalyze Trp degradation to kynurenine metabolites. In metabolomics, Trp was lower (1.33-fold) in plasma of AD patients compared with cognitively normal (CN) individuals.[45] High TDO and IDO likely reduce Trp level resulting in increase of tryptamine/Trp ratio in hippocampus.

Skatole

A lower mean level of skatole (1.4-fold) is detected for C&A compared with NNI. In C&A, a highest skatole value is detected in obese/T2D individual (+antibiotics) and a lowest is for a less obese individual with T2D (–antibiotics).

Indolepropionic acid

Indolepropionic acid show lower (1.23-fold) levels in C&A (34 samples) compared with NNI (22 samples). Statistically significant difference in Trp/IPA ratio ($P < .0001$) was found between NNI (6.1-fold) and C&A (6.8-fold). The values for three individuals with a high identity to ADAS are in the lower 50% of IPA values in both populations. Indolepropionic acid protected the primary neurons and neuroblastoma cells against oxidative damage and death caused by exposure to amyloid β.[46]

Indole-3-carboxylic acid

Indole-3-carboxylic acid was detected in 4 of 23 NNI samples (17.39%) and 12 of 38 C&A samples (31.58%). Two high ICA values were detected for C&A obese/T2D, while one of two has a high identity to ADAS. The significantly lower ICA values (3.7-fold, two-tailed *P*-values) were found in C&A population (10 participants) compared with three of four NNI. Indole-3-carboxylic acid has been detected in bacteria, yeast,[47] and pathogenic fungus.[48] Indole-3-carboxylic acid was detected in uremic patients[49] and has been found elevated in patients with liver diseases. Indole-3-carboxylic acid is a mediator of priming against plant necrotrophic pathogenic fungus *Plectosphaerella cucumerina*.[50]

Peptides altered in C&A vs NNI

The Cheyenne and Arapaho values for tripeptide Leu-Leu-Leu and dipeptide Leu-Gly show a higher level (2-fold and 1.3-fold, respectively) compared with NNI (Table 2). A higher level of dipeptides may indicate a higher proteolysis in C&A. Since NNI group includes no T2D, the C&A T2D subgroup is compared with NNI. Tryptophan- and methionine- (Met) dipeptides (Table 2; Figure 1) show lower levels in C&A compared with NNI: Trp-Pro (–1.8 fold), Trp-Val (–1.1 fold), and Met-Val (–1.2 fold). Most probably, the aminoacyl-tRNA deficiency resulted in the dipeptide decrease. Inhibition of tRNA aminoacylation in gut microbes can lead to dysbiosis (Figure 4). Present meta-analysis detects a trend toward the reduction

in presumably rare Trp-and Met-containing dipeptides and elevation of Leu-dipeptides in C&A compared with NNI. A critical role of tRNA aminoacylation deficiency with consequent protein biosynthesis impairment is supported by decrease in the levels of di- and tripeptides in AD plasma compared with mild cognitive impairment (82.8-fold decrease of Met-His-Lys in AD) and CN.[45] The present meta-analysis indicates that tRNA aminoacylation impaired in gut microbiome of a group with a high prevalence of AD-associated diseases.

Alzheimer disease-associated sequence in morbidly obese (Denmark); obese with non-alcoholic fatty liver disease (NAFLD) and inulin diet (Germany); atherosclerosis (Sweden); Western and Korean diet (Australia); Parkinson disease (PD, Germany); bacterial strain (healthy, UK); inflammatory bowel disease (IBD); and fecal transplantation

Denmark. Alzheimer disease-associated sequence was found in stool samples from 3 out of 13 morbidly obese patients at 100%, 97%, and 89% nucleotide identity. Study participants were recruited at Hvidovre Hospital, Denmark, as a part of the bariatric surgery program.[51] Danish criteria for bariatric surgery are as follows: (1) >20 years of age and (2) either body mass index (BMI) >40 kg/m^2 or >35 kg/m^2 with T2D/hypertension. In an Austrian study of 22 morbidly obese individuals and 20 normal-weight volunteers, the serum Trp levels were significantly lower in morbidly obese patients (preoperative: 51.5 ± 9.2 μmol L^{-1} and postoperatively, bariatric surgery: 46.9 ± 7.6 μmol L^{-1}) when compared with those of normal-weight controls (64.8 ± 9.5 μmol L^{-1}, $P < .001$).[52] In the US study of serum metabolites in obese patients,[53] IAA (0.51-fold), IPA (0.38-fold), Trp (0.63-fold), Tyr (0.62-fold), and Phe (0.69-fold) are significantly lower in obese patients with T2D compared with baseline.

Germany (inulin diet). Alzheimer disease-associated sequence was found at 88% nucleotide identity in 3 of 16 patients (18.7%) in the study conducted by the University of Hohenheim, Germany (NCBI accession no. PRJNA290729). To gain insight into connection between microbiota, obesity, and diet, the gut metagenome of 16 patients was analyzed following a weight-loss program based on a very low-calorie inulin-enriched formula diet. Alzheimer disease-associated sequence was found in stool samples of three patients only after the inulin diet. An increase was observed in the fecal concentrations of tryptamine (2.5-fold, $P < .05$) and tyramine (2-fold, $P < .05$) following the inclusion of inulin (3 g/kg of body weight per day) in the equine diet.[54] All three obese patients with ADAS have NAFLD. It is well established that advanced forms of liver disease are frequently accompanied by overt and global cognitive deficits in hepatic encephalopathy (HE).[55] Findings of decreased densities of [3H]tryptamine binding sites in brain tissue from cirrhotic patients with HE taken in conjunction with reports of increased cerebrospinal fluid and brain tryptamine concentrations in HE suggest a pathogenic role for tryptamine in HE resulting from chronic liver failure.[56] Hepatocellular death is present in almost all types of human liver disease and used as a sensitive parameter for the detection of acute and chronic liver disease. Clinical data and animal models suggest that hepatocyte death is the key trigger of liver disease progression.[57] Electroencephalographic rhythms reveal larger spatial-frequency abnormalities in liver cirrhosis patients with a cognitive impairment due the covert and diffused HE compared with AD.[58] A cerebellum of patients with steatohepatitis, a type of fatty liver disease, shows loss of Purkinje and granular neurons.[59]

Sweden. Alzheimer disease-associated sequence at 89% nucleotide identity was found in 2 of 12 patients with atherosclerosis and in 1 of 13 controls. The patient stool samples were from the Göteborg Atheroma Study Group Biobank, which includes samples from patients who had undergone surgery to excise an atherosclerotic plaque.[60]

Australia. Alzheimer disease-associated sequence was found at 89% nucleotide identity in 3 (fecal microbiota study EKmeta) of 12 participants at two time-points of the two diets—Korean and Western. Each group included six individuals, half of which loose high weight and half of which loose little weight. Fecal samples were collected before and after diet (3 months). Alzheimer disease-associated sequence was found in two individuals only before Western diet/high weight loss and in one only after Western diet/high weight loss.

Germany (Parkinson disease). The 72% to 75% nucleotide sequence identity to ADAS was observed in 8 of 31 early-stage, L-3,4-dihydroxyphenylalanine (DOPA)-naive PD subjects and in 3 of 28 control individuals of gut microbiome study conducted in Germany.[61] Nucleotide sequences with a high identity (89%-99%) to the nucleotide sequence prevailed in PD are frequent in the control dbGaP study (100 of 300). Alzheimer disease-associated sequence at 88% nucleotide identity revealed in one control stool sample of this PD study (Supplemental Table S1). Therefore, no high identity to ADAS reveled in stool samples of PD patients.

Inflammatory bowel disease, irritable bowel syndrome, and fecal transplantation

Here, the 89% nucleotide sequence identity to ADAS was found in donor fecal transplant for treatment of recurrent Clostridium difficile infections[62] and in stool sample of active Crohn disease (CD) patient following fecal transplantation.[63] The 89% identity to ADAS was also tracked in other CD and ulcerative colitis (UC) patients with IBD in the United States with no fecal transplantation. In a Korean study, tryptamine (3×, $P = .01$) is among the significantly different fecal metabolites between irritable

Table 3. Blood glucose level, weight progression, and positron emission tomography studies of glucose utilization (standardized unit values) in control and tryptamine-treated mice.[12]

VALUES	CONTROL ANIMALS (N = 6)	TRYPTAMINE TREATED (N = 6)
Blood glucose (mg/dL)	138 ± 19	129 ± 19
Weight progression (%)	11.4 ± 4.5	20.8 ± 3.8
Glucose utilization		
Whole brain	0.94 ± 0.11	0.95 ± 0.18
Cerebellum	0.72 ± 0.12	0.68 ± 0.07
Cingulate	1.29 ± 0.10	1.27 ± 0.13
Hippocampus	1.24 ± 0.11	1.17 ± 0.17
Olfactory area	1.43 ± 0.21	1.36 ± 0.13
Striatum	1.21 ± 0.12	1.17 ± 0.16

Table modified from Paley et al.[12] Tryptamine-treated mice: after tryptamine administration of 200-400 µg per mouse through intraperitoneal injections during 63 days[12].

bowel syndrome (IBS) patients and non-IBS controls identified by GC-MS.[64] Serum levels of Trp were significantly lower in patients with IBD than in controls.[65] The IBD pathology likely includes the recently demonstrated activation of epithelial G-protein-coupled receptor by gut microbiota-produced tryptamine that increases colonic secretion.[66]

Alzheimer disease-associated sequence-containing bacteria in healthy subjects: United Kingdom, Canada (antibiotics), and the United States

Alzheimer disease-associated sequence at 89% identity was found in nucleotide sequence (~40 kbp) of the cultured spore-forming unclassified bacteria (SFB) from the gut microbiome UK study of six healthy individuals.[67] Spore-forming bacteria at 99% nucleotide identity presents in nucleotide fragments from three healthy subjects (~5.8, 3.5, and 2.3 kbp length, respectively) of Canadian study[68] after treatment with antibiotic (Supplemental Table S1). In this study (24 subjects), stool samples gathered before antibiotic exposure, at the end of the treatment and 3 months later, were analyzed using shotgun metagenomic sequencing. The spore-forming bacteria appeared only at 3 months after the treatment in all three subjects. The 99% nucleotide identity to SFB was detected in ~1000 to 7500 bp fragments from 4 subjects out of 300 healthy individuals (dbGaP study). Shorter nucleotide sequences (200-600 bp) with 99% identity to SFB are more frequent (8 subjects) in dbGaP. Genome assembly is typically a two-stage process: contig assembly followed by the use of paired sequencing reads to join contigs into the scaffolds at the last step, the gap-filling stage. In the eight subjects, scaffolds for ADAS$^+$ SFB are short. Spore-forming bacteria with a considerable sequence length presents in 1 of 300 from dbGaP study. Spore-forming bacteria show 99% nucleotide identity (E = 0.0) to uncultured ADAS+ *Clostridium sp.* from stool sample of obese person.[1]

Tryptamine in weight progression and glucose metabolism in mice

We demonstrated that a 2-month tryptamine treatment through intraperitoneal injections induces weight progression in mice. The 2-fold higher weight progression was detected in six tryptamine-treated mice compared with six control mice similarly treated with placebo. Weight progression (%) was detected at 11.4 ± 4.5 in control mice vs 20.8 ± 3.8 following tryptamine treatment. In addition, tryptamine alters glucose concentrations in blood and brain including hippocampus (Table 3) monitored by 18 F-fluorodeoxyglucose (18 F-FDG) positron emission tomography (PET).[11] Blood glucose (mg/dL) was detected at 138 ± 19 in control mice and at 129 ± 19 in tryptamine-treated mice.[11] Hypoglycemia most likely occurs in people with pre-diabetes. PET studies show 18 F-FDG utilization difference in hippocampus at 1.24 ± 0.11 in control vs 1.17 ± 0.17 in tryptamine-treated mice.[12] PET imaging of 18-FDG reduced glucose metabolism in hippocampus has been successfully used for AD monitoring.

Tryptamine induce WARS gene-dose dependent effects

Tryptamine (50 µg/mL) is cytotoxic for HeLa cells with LD_{50} at 100 µg/mL (Figure 2). Tryptamine treatment significantly reduced the TrpRS gene (WARS) hybridization of DNA from human HeLa and hamster 631 cells.[7] These data indicate that tryptamine affects HeLa and 631 cells in a gene-dose dependent manner (Figure 2). Similarly, the reduced TrpRS gene copy number results from the inhibition of DNA polymerase protein

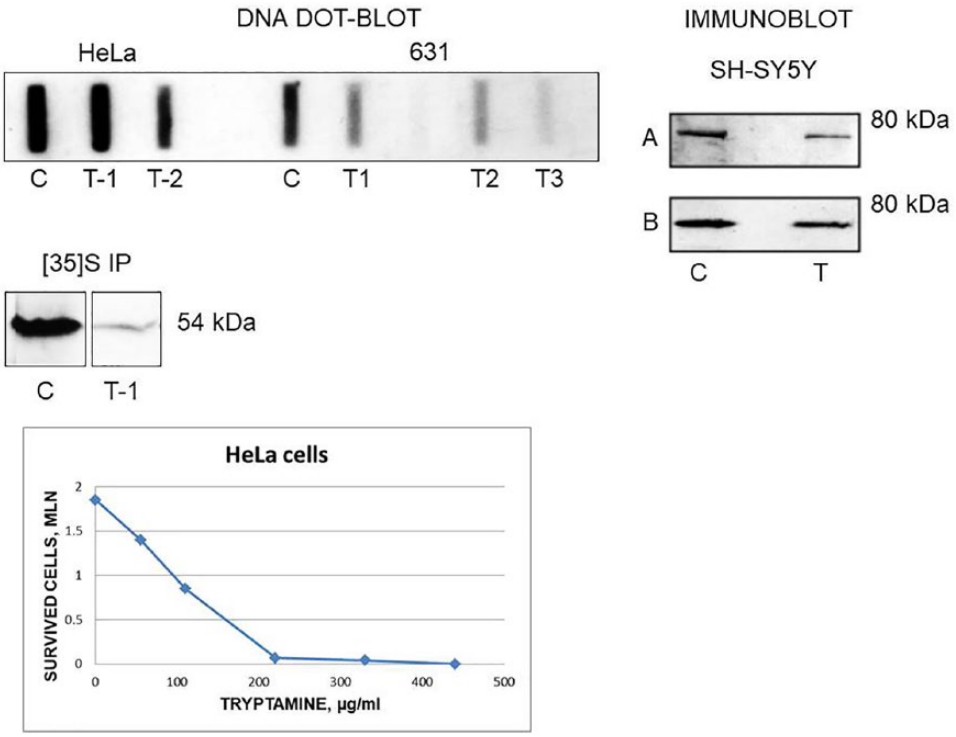

Figure 2. Tryptamine induces the WARS gene-dose dependent effects. DNA—DNA dot-blot analysis of human HeLa and hamster 631 control (C) and tryptamine-treated (T) cells using WARS gene probes. [^{35}S]IP—immunoprecipitation of [^{35}S]methionine labeled HeLa cells with polyclonal antibodies to TrpRS. Immunoblot—immunoblotting of human neuroblastic cells SH-SY5Y with anti-TrpRS monoclonal antibodies 6C10; A—total extract, B—detergent-soluble fraction. HeLa cells—a dose-dependent cytotoxic effect of tryptamine. Note, similar images published as parts by the author in different context. This figure includes the images obtained and redesigned here by the author as the own data revisiting and revision.[7,12] To support the newly presented concept based on the recent works, the author combined these data together. Specifically, the author presents here for the very first time the interpretation of the DNA dot-blot results as the evidence of WARS gene-dose dependent cytotoxicity. This new conclusion is of considerable interest for understanding a mechanism of neurodegeneration induced by tryptophan metabolites, the TrpRS inhibitors. The tryptamine-treated HeLa T-1 possess WARS gene variant encoding TrpRS with a longer half-life compared with TrpRS from original HeLa cells; T-1 has a slower growth rate compared with HeLa.[7] The tryptamine-treated sublines HeLa T-2 and 631 (T1, T2, and T3) possess WARS gene at a lower dose compared with original cell lines.

biosynthesis by tryptamine. Tryptamine-induced decrease in TrpRS protein abundance is detected by immunoprecipitation of HeLa[7] and by immunoblotting of SH-SY5Y[12] cells with anti-TrpRS antibodies. These data are in agreement with the decrease in electron microscopy density of RNA polymerase on promoter-distal portions of cloned Trp operons of *Salmonella typhimurium* induced by TrpRS inhibitor indoleacrylic acid.[69] Tryptamine suppressed DNA synthesis in the presence of rat liver S9 tissue homogenate.[70] DNA polymerase β deficiency leads to neurodegeneration and exacerbates AD phenotypes.[71] Thus, tryptamine diminishes TrpRS abundance and activity. Quantitative transcriptomics of the tissue-specific expression of genes across a set of 27 human organs and tissues demonstrates that WARS gene expresses differentially in human organs with a highest expression in placenta (mean reads per kilobase million [RPKM] = 128.2) and appendix (RPKM = 87.1) and a lowest expression in pancreas (RPKM = 3.2) and colon (RPKM = 31).[72] Similarly, human organs have differential sensitivity to TrpRS inhibitors—pancreas and colon—high and placenta low. Tryptamine-induced chromosomal rearrangements and TrpRS gene mutations can also be implicated in neurodegeneration. Earlier, we found chromosomal rearrangements in bovine kidney[4] and hamster[13] cells following prolonged tryptamine treatment. In tryptamine-resistant SV40-transformed Djungarian hamster DM 15 fibroblasts, the Giemsa banding showed additional material in the short arm of one homologue of chromosomes five and seven in 40% and 80% of cells, respectively. Small double-minute chromosomes were detected (1-2 per cell) in 5% of cells.[13] Stacking interaction of tryptamine with nucleic acid base and 3-methylcytidine-5′-monophosphate:tryptamine complex (crystal structure)[73] can result in a single nucleotide polymorphisms (SNPs). In a Finnish cohort, AD is associated with SNPs.[74] Biallelic mutations in the mitochondrial TrpRS gene (WARS2) cause decreased WARS2 protein and Parkinsonism.[75] The reported data related to tryptamine-induced chromosomal and gene abnormalities are summarized in Supplemental Table S2.

Tryptophanyl-tRNA synthetase in AD brain blood vessels

Figure 3 shows the cerebral vascular cells of AD human brain vasculature immunostained by mAb 9D7 against TrpRS. In the superior frontal gyrus (frontal lobe), a strong abnormal TrpRS immunostaining of the cell periphery shows the likely dysfunctional vascular endothelium. Normally, TrpRS immunostaining

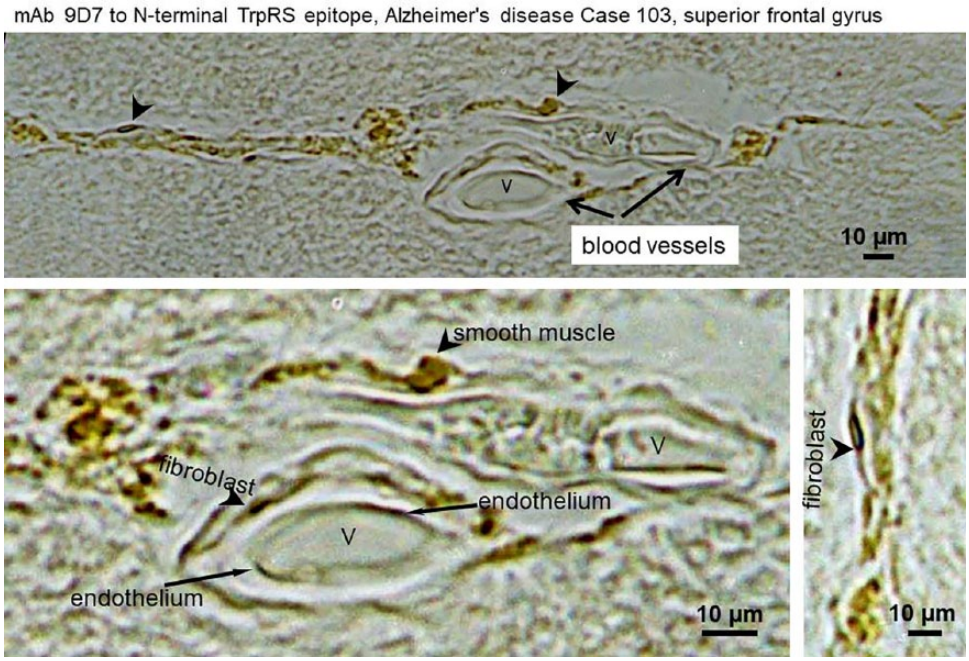

Figure 3. Immunostaining of cerebral blood vessels in AD superior frontal gyrus brain section with monoclonal antibodies 9D7 to TrpRS. Arrows indicate endothelial, fibroblast, and smooth muscle cells. The letter "V" shows the vessels. Scale bars: 10 µm.

is diffused in the light and electron microscopy since this enzyme is mainly cytosolic.[4,6] Plausibly, TrpRS of the vascular endothelium including fibroblasts, smooth muscle, and endothelial cells (Figure 3) is a target of tryptamine cytotoxicity, which can lead to necrosis and holes in the blood vessels of brain and other organs and tissues. The AD cerebral amyloid angiopathy of grade 3 is a cracking of ⩾50% of the circumference of the vessel, and grade 4 is fibrinoid necrosis of the vessel wall.[76] Fibrinoid necrosis also occurs in the vascular walls in hypertension.[77,78] Tryptamine is a vasoconstrictor in umbilical vessels of the human placenta,[79] in renal circulation, and vessels of the ear (doses 5-10 µg)[80] inducing hypertension.[81] The tryptamine vasoconstriction is modulated by the co-released endothelial vasodilator, nitric oxide.[82] Generally, vasoconstriction results in an increase in systemic blood pressure, but it can cause a localized reduction in blood flow. Tryptamine, tyramine, and PEA from the equine cecum were potent constrictors of arteries and veins.[83] Infusion of tryptamine (1-4 µg/mL) through the pulmonary circulation of isolated lungs caused release of spasmogens contracting smooth muscle preparations.[84] The holes in the blood vessels can lead to bleeding stopped by coagulation and clot formation. Tryptophanyl-tRNA synthetase co-localizes with amyloid-β in cerebral blood clot-like formations in AD brain.[5] Clinical studies have demonstrated the blood-brain barrier dysfunction in AD patients exhibiting peripheral vascular abnormalities such as hypertension, cardiovascular disease, and diabetes.[85] The anatomo-physiological route/s for microbial tryptamine from gut to brain and other organs remains unknown. The vasculopathies in AD and in tryptamine-treated mice[5] may result in anatomical loop, drainage, or siphoning in transporting microbial tryptamine from gut to organs such as pancreas and brain. Transport of gut microbial tryptamine can be redirected from the normal route to liver due to (1) portal vein thrombosis (blockage or narrowing of the portal vein—the blood vessel that brings blood to the liver from the intestines) by a blood clot[86]; (2) deposits in portal vein or portal amyloid[87]; (3) congenital portosystemic venous shunt (CPSS),[88] which is a rare developmental anomaly resulting in diversion of portal flow to the systemic circulation.[89] CPSS are rare vascular anomalies occurring secondary to abnormal development or involution of fetal vasculature. They allow intestinal blood to reach the systemic circulation bypassing the liver, resulting in a variety of symptoms and complications in the longer term. Children with CPSS may present with unexplained neurocognitive dysfunction and other behavioral issues due to low-grade HE, and this accounts for 17% to 30% of cases. Other manifestations include learning disabilities, extreme fatigability, seizures, and failure to thrive. The likelihood of encephalopathy increases with age and is related to the shunt flow[89]; (4) in the study of the three-dimensional (3D) arrangement of the entire brain of AD transgenic (tg) mice vasculature, at young ages, the APP23 tg mice had significant alterations, particularly of the microvasculature, often accompanied by small deposits attached to the vessels. In older animals, vasculature abruptly ended at amyloid plaques, resulting in holes. Often, small deposits were sitting near or at the end of truncated vessels. Between such holes, the surrounding vascular array appeared more dense and showed features typical for angiogenesis[90]; and (5) in our study, tryptamine induce vasculopathy in cerebral amyloid angiopathy and angiogenesis with increased vascular density in the hippocampus of mouse brain.[5] In the hippocampus of AD

Table 4. ADAS in CRC studies.

PARTICIPANTS	CHINA CONTROL	CHINA CRC	USA CONTROL	USA CRC
Total, N	54	74	52	52
ADAS (88%), N	1	6	0	14
ADAS (100%), N	0	0	1	0
ADAS prevalence, %	1.85	8.1	1.9	27

Abbreviations: ADAS, Alzheimer disease-associated sequence; CRC, colorectal cancer; N, number of participants.

postmortem brain, the ongoing angiogenesis result in increased vascular density compared with controls.[91]

Alzheimer disease-associated sequence, tryptophanyl-tRNA synthetase, tryptamine, dipeptides in colorectal cancer

Present BLAST search of NCBI databases discovers that ADAS prevails in CRC (Table 4) of the two human gut microbiome studies (China[35] and Washington, DC[92]).

Low TrpRS expression in tumors correlates with increased risk for recurrence and worse survival in patients with CRC.[93] Furthermore, increased risk of lymph node metastases and a more advanced tumor stage were identified for patients with a low TrpRS expression. In CRC stage-I group, 15 of 30 cases were positive for IDO. The four patients from a high IDO (presumably low Trp) expression group had distant metastases.[94] Tryptophanyl-tRNA synthetase and IDO are interferon-inducible proteins. Earlier, we demonstrated that down-regulation of full-length TrpRS by hypoxia is concomitant with a higher metastatic ability of human pancreatic cancer cells.[6] Therefore, a low TrpRS expression is a characteristic feature of tryptamine-induced neurodegeneration and metastatic cancer. Alzheimer disease comorbidities among older adults (⩾60) included metastatic cancer.[95] Here, fecal metabolites from Washington, DC study of 48 CRC cases and 102 matched controls were compared in terms of prevalence (%) as a fraction above the detection limit. Tryptamine was detected in 65% of CRC cases and 60% of controls; ICA 92% (CRC) vs 75% (control); dipeptides tryptophanyl-isoleucine 85% (CRC) vs 97% (controls); valyl-Trp 88% (CRC) vs 92% (controls); threonyl-arginine 71% (CRC) vs 80% (controls); valyl-arginine 75% (CRC) vs 80% (controls); tyrosyl-tyrosine 94% (CRC) vs 99% (controls); methionyl-alanine 60% (CRC) vs 64% (controls); lysyl-proline 96% (CRC) vs 100% (controls); anthranilate (precursor to Trp) 100% (CRC) vs 97% (controls); and 2,8-quinolinediol 73% (CRC) vs 89% (controls).[96] A lower abundance of 2,8-quinolinediol was also observed in C&A compared with NNI (Supplemental File 1). Lower abundance of dipeptides in CRC (35% with metastases at diagnosis) compared with mucosa was also detected in the other CRC study for tryptophanyl-glycine (0.84-fold), aspartyl-valine (0.81-fold), and aspartyl-Trp (0.76-fold).[97] In summary, a higher frequency of ADAS detection correlates with a higher tryptamine detection frequency and lower detection of some dipeptides including Trp-containing dipeptides in CRC compared with controls. Although CRC is not a classic cell death-related disease, the tumor necrosis was observed in 365 (96%) CRC cases in the Austrian study.[98] Extent of necrosis was significantly associated with blood vessel invasion and large tumor size. These data indicate that blood-borne cytotoxic mitogen presents in CRC tumors (Figure 4).

Common characteristic pathophysiological features of AD and ADAS/tryptamine-associated diseases

This study shows a presence of ADAS in Native American population with a high percentage of obesity and T2D. The adipocyte hypertrophy occurs during weight gain and is associated with recruitment of immune cells, mainly adipose tissue macrophages (ATMs), into the adipose tissue (AT). The ATM cells typically surround a dying or dead adipocyte with the formation of crown-like structures (CLS) that are present in experimental models of obesity and in obese individuals.[99] Adipose tissue macrophage undergoes mitosis within AT, predominantly within CLS.[100] Tryptamine elicited a concentration-dependent mitogenic response in smooth muscle cells (ED_{50}, 0.8 μM).[9] Previous report documents that tryptamine exerts both cytotoxic and mitogenic activities toward cell variants (cancer stem cells) of human neuroblastic cell line SH-SY5Y.[8] The neuronal cell cycle-reentry has been extensively evidenced in AD brains.[101] Confocal laser microscopy visualized the hippocampal dividing neurons in AD brain.[8] Cancer is associated with a reduced AD risk[102] but AD directly linked to CRC. Likely, the primary targets of the human gut microbial tryptamine cytotoxicity are gut microbes[20,21] and human intestinal cells including epithelium. The gut bacterial TrpRS inhibition by microbial Trp metabolites including tryptamine, tryptophanol, and IAA[5] most likely lead to dysbiosis/impaired microbiota. The sensitivity of yeasts to tryptamine is strain-dependent.[24] Thus, tryptamine plays a role of selective factor in evolution of human gut microbiome. Intestinal cells are damaged in UC patients who had overall mortality comparable to the general population, though being at increased risk of dying from Hodgkin disease, rectal cancer, and AD.[103] Ulcerative colitis is the IBD that causes long-lasting inflammation and ulcers (sores) in mucosa of the digestive tract. The pathogenesis of IBD includes increased intestinal epithelial cell death, altered expression, and distribution of tight junction proteins, along with a decreased expression of antimicrobial peptides and disruption of intestinal barrier integrity.[104] Tryptamine increase (1.38-fold) was found in human saliva of patients with recurrent aphthous ulcer (RAU) compared with healthy controls.[105] Recurrent aphthous ulcer is associated with IBD.[106]

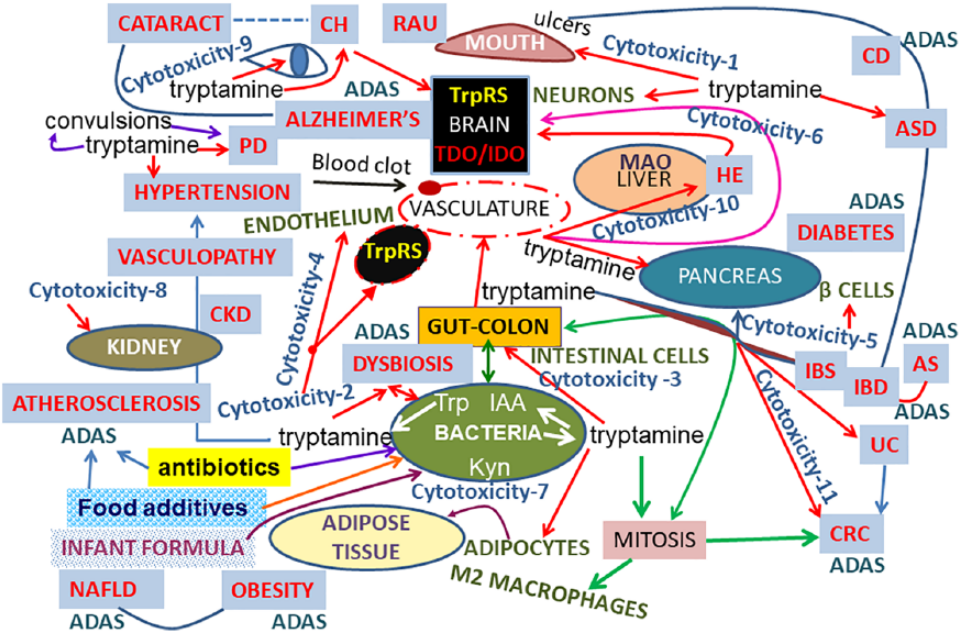

Figure 4. The scheme of the common characteristic features of AD and related diseases: crosstalk between disease-associated ADAS and tryptamine. This figure summarizes and illustrates the complex effects of tryptamine (cytotoxic and mitogenic), tryptamine role in different human cells, organs, health conditions, and cell death diseases, and a link of tryptamine to ADAS. This scheme combines our data reported here for the first time, our previously reported results, and the present analysis of multiple studies of other authors. The details of the scheme, references, and abbreviations are included in the "Results and discussion" section and Supplemental.

Abbreviations: TrpRS, tryptophanyl tRNA synthetase; MAO, monoamine oxidase; ADAS, Alzheimer's disease associated sequence; CRC, colorectal cancer; Trp, tryptophan; IDO, indoleamine-2,3-dioxygenase; IAA, indole-3-acetic acid; Kyn, kynurenate; TDO, tryptophan 2,3-dioxygenase; NAFLD, non-alcoholic fatty liver disease; IBD, inflammatory bowel disease; UC, ulcerative colitis; CD, Crohn's disease; AS, ankylosing spondylitis; HE, hepatic encephalopathy; RAU, aphthous ulcer; IBS, irritable bowel syndrome; PD, Parkinson's disease; CKD, chronic kidney disease; ASD, autism spectrum disorders; CH, chronic cluster headaches.

Patients with IBD may present with these oral manifestations years before the appearance of intestinal disease. Association between IBD and CRC has been recognized since 1925 and still accounts for 10% to 15% of deaths in IBD.[107] Cognitive impairment and RAU were detected in another IBD, the CD.[108] The UC patients typically present with rectal bleeding probably caused by peripheral vasculopathy. Alzheimer disease-associated sequence at 88% nucleotide identity was found in stool samples of UC and CD patients. In the China study of 97 patients with AS and 114 healthy controls,[109] AS patient reveals 100% nucleotide identity to ADAS. Ankylosing spondylitis and IBD shared similar genetic risk factors and etiopathogenesis. A multitude of diseases including IBD, obesity, T2D, and AD are associated with intestinal dysbiosis. Secretion of bacterial toxins such as tryptamine can trigger rapid shifts among intestinal microbial groups thereby yielding dysbiosis. A common feature of AD, diabetes, obesity, IBD, and liver diseases are cell death and diet-dependent ADAS/tryptamine abnormalities (Figure 4; Supplemental Tables S3 and S4). Some antibiotics cause dysbiosis with consequent tryptamine overproduction in gut. Centers for Disease Control and Prevention (CDC) estimates that in 2015 alone, approximately 269 million antibiotic prescriptions were dispensed from outpatient pharmacies in the United States, enough for five out of every six people to receive one antibiotic prescription.

Alzheimer disease-associated sequence and tryptamine in infants

In the European study InfantGut, samples of nine mothers (shortly after birth) reveal 88% identity to ADAS. Samples of mothers, their infants at birth, 4 months, and 12 months were collected for InfantGut study (400 samples). Alzheimer disease-associated sequence at 88% identity was detected in stool samples of four 12 month-old infants.[110] One infant showed 98% nucleotide identity to ADAS from the mother. The 13.3% of mothers had antibiotics during labor and 24.5% of infants had antibiotics at 12 months. In the United States, the 93% nucleotide identity to ADAS was observed in 1 infant (83.4 day of life male) of 84 (prevalence = 1.19%) longitudinally sampled preterm infants in neonatal intensive care unit (St. Louis, MO).[111] Preterm infants almost universally receive early and often repeated and/or prolonged intravenous antibiotic therapy.

Food additives pectin and fructooligosaccharides increase (Supplemental Table S3) fecal tryptamine.[112] During 3 weeks, a formula diet for infants switches the gut microbiome production from serotonin to tryptamine in piglets (2 days old) relative to breast-fed piglets (sow-fed).[113] Tryptamine colon contents were higher for infant formula-fed piglets (~80 μg/mg) compared with breast-fed (~40 μg/mg) piglets. A diet milk-formula contained much lower tryptamine of ~0.02 μg/mg and sow <0.01 μg/mg. Thus, the sow-fed piglets showed the tryptamine colon contents that can be cytotoxic for both microbial and mammalian cells.

Likely, the piglets acquired the tryptamine-producing microbes from mother and/or environment within the first 3 weeks of life. In human fecal non-targeted metabolomics, out of seven BA, only single amine, tryptamine, was significantly higher (1.85-fold) in formula-fed than breast-fed infants of 2 to 4 months.[114] These data support a diet-dependent role of microbial tryptamine in the early-life gut dysbiosis.

Tryptamine in cataract

Tryptamine is higher in human senile cataractous lenses (0.2-2.78 μg/g) than in non-cataractous lenses (0.06-0.48 μg/g).[115] Infection occurs before and after cataract surgery. The primary source of intraocular infection is considered to be bacteria from the patient's ocular surface (cornea and conjunctiva) or adnexa (lacrimal glands, eyelids, and extraocular muscles).[116] Tryptamine-producing bacteria can be a source of tryptamine in cataractous lenses. In the epithelium of lens from cataract patients, a cell death was observed.[117] Degeneration and transdifferentiation of human lens epithelial cells were found in cataracts.[118] Tryptamine induce cell degeneration and transdifferentiation.[7] Older people with cataract are at increased risk of developing AD.[119]

Tryptamine in adult healthy humans, Parkinson disease, chronic cluster headache, and children with autism spectrum disorders

Microgram quantities of fecal tryptamine were detected in healthy humans (mean value = 2.00 ± 1.24 μmol/g dry matter or ~160-480 μg/g) similar to tryptamine microgram content in animal stool samples.[5,120] The amounts of tryptamine in human stool samples from C&A range between 19 163 and 3 121 278 units in the present meta-analysis of the reported crude data.[29] Retrospectively, I re-examined the original unpublished crude data on high-performance liquid chromatography (HPLC) tryptamine detection in 68 healthy human stool samples (mean age = 26.2 years, weight = 70.9 kg). Large inter-individual variations of fecal tryptamine contents revealed in the healthy humans (Supplemental Figure S1) in agreement with the reported data.[120] The highest fecal tryptamine values above 400 μg/g revealed in 16 individuals, above 600 μg/g in 7 subjects, and above 800 μg/g in 3 participants, while the lowest values below 200 μg/g were detected in 18 subjects. Similar mean value of fecal tryptamine 0.16 ± 0.4 mg/g of wet fecal sample was detected by BA-targeted LC-MS/MS in non-autistic siblings (n = 35, 2-12 years of age) of children with autism spectrum disorder (ASD) aged 2 to 12 years in Australia.[41] Based on the provided SD values, the inter-individual variation in the fecal tryptamine mean values was estimated here to be 0.072 to 0.56 mg/g. In this study, the mean fecal tryptamine values were 4-fold higher for severe (n = 16) autism (0.16 ± 0.44) compared with mild (n = 19) autism (0.04 ± 0.16). A high mean tryptamine level detected in siblings of ASD children can be explained by reported depression, bipolar disorder, and psychiatric disorder, which occur more frequently in family members of individuals with ASD than in the general population.[121] Reduced pyramidal neuron size was found specifically in children with autism aged 4 to 8 years.[122] A higher prevalence of CD and UC in ASD children compared with controls confirms the association of ASD with IBD.[123]

Urinary tryptamine concentration progressively increased during the day and continued to increase during the night when subjects were asleep in 14 healthy male volunteers.[124]

Mass spectrometry metabolomics of 401 urine samples from 106 idiopathic PD patients and 104 normal subjects demonstrated 3.3-fold tryptamine increase in PD.[125]

The plasma levels of tryptamine were found several times higher in chronic cluster headache (CH) patients (23 participants) compared with controls (28 individuals).[126] Morphometry reveals that migraine is associated with a significant gray matter reduction in several of the cortical areas involved in pain circuitry.[127] Cases of cataract in CH were reported.[128] Chronic cluster headache was reported as a first manifestation of multiple sclerosis.[129]

Tryptamine appeared in increased concentrations in the urine before and during the activation of psychotic symptoms that could by associated with tryptamine psychotomimetic metabolite N,N-dimethylated tryptamine.[130]

Monoamine oxidase inhibitors

The two MAO forms, MAO-A and MAO-B, contribute to the metabolism of tryptamine in human tissues.[131] The highest levels of human MAO-A and MAO-B were measured in liver and lowest in spleen.[132] Different organs show distinct expression patterns for MAO[133] controlled by a variety of factors including DNA methylation of MAO gene.[134] Monoamine oxidase inhibitors (MAOIs) act by inhibiting the activity of MAO, thus preventing degradation of monoamine tryptamine. Gas-chromatographic analyses, either alone or in combination with MS, of tissue from rats treated with antidepressants (MAOI) indicated increased brain tryptamine levels in several studies.[135] Intoxications with MAOI tranylcypromine (TCP) are fatal for human.[136] The highest survived TCP-dosage was 4000 mg and the lowest fatal dosage was 170 mg. Because of the large difference between the survived and the lethal TCP dosages, it is suggested that the individual susceptibility factors such as individual concentrations of toxic tryptamine might play a role in the severity of clinical symptoms independent of the ingested TCP dosage. Abnormal pregnancy outcome including fetal death and dysmorphism is associated with high-dose maternal TCP therapy.[137] The poisoning was described for 35 cases with TCP usage and 56 cases with usage of MAOI phenelzine, which is one of the few non-selective and irreversible MAOIs still in widespread clinical use.[138] Sixty to 75 seconds after intravenous injection of non-convulsive

dose of tryptamine (5 mg/kg), brain concentration of the amine tryptamine was increased 5.4-fold. Occurrence, duration, and relative intensity of clonic convulsions produced by injection of tryptamine into rats pretreated with TCP (oral administration of 0.72 mg/kg) were correlated with increased concentration of tryptamine in the rat brain.[139] The 34-fold tryptamine increase in rat hippocampus induced by TCP was administered at 20 mg/kg intraperitoneally.[140] In six healthy human volunteers, urinary tryptamine increased up to 7-fold, dose dependently with large inter-individual variation (78 ± 27 to 549 ± 252 µg/g creatinine) once the cumulative dose of 40 mg TCP had been administered.[141] In six healthy human volunteers, blood pressure sensitivity to intravenous tyramine increased 2.6-fold during phenelzine (60 mg/day), whereas sensitivity to oral tyramine increased 15.7-fold. Urinary elimination of tryptamine increased during phenelzine (antidepressant) to 12.7-fold.[142] Although tryptamine is a MAO substrate, it is also a MAOI precursor in the reaction of Pictet-Spengler condensation of aldehydes with tryptamine to form β-carboline alkaloids[143,144] inhibiting MAO.[145] Clearly, the exogenous MAOI and endogenous tryptamine-derived MAOI can potentiate the tryptamine toxicity.

Decontamination of gut microbial tryptamine by activated charcoal

In chronic kidney disease (CKD) patients with CKD progress to end-stage renal disease, the fecal tryptamine is 2.62-fold higher in hemodialysis (HD) patients compared with controls (20 healthy controls and 31 HD patients) and became lower in HD patients than in controls (0.18-fold) after taking medicinal charcoal tablets AC (activated charcoal) for 3 months[146] (Supplemental Table S4). The two most common causes suggested for kidney disease are diabetes and high blood pressure. Indole-3-acetic acid, a product of tryptamine degradation catalyzed by MAO, is an uremic toxin accumulated in HD patients with CKD.[147] In our study, tryptamine induced degeneration and cell death in bovine kidney cells.[4] Due to its strong adsorption ability, AC has been used in CKD patients to reduce serum uremic solute. *E coli* strains producing verotoxin were also effectively adsorbed by AC.[148] Manic episode associated with delusional ideas and hallucinations of obese patient was resolved 15 days after beginning the treatment with AC.[149] The manic episode occurred 15 days after the patient undergone subtotal gastrectomy for morbid obesity. Iodinated AC significantly improved lung function of patients with moderate chronic obstructive pulmonary disease in 8 weeks treatment while AC was used as placebo in the control group.[150] After ingestion of a potentially toxic substance, single-dose AC is the most applied gut decontamination procedure. In short, it is easy to use, inexpensive, and safe.[151]

Conclusions

It becomes evident that ADAS used as a query in the search of NCBI databases enabled to uncover a link of AD-associated gut bacteria with obesity, T2D, CRC, NAFLD, and IBD. This study supports a model of tryptamine-induced diseases, in which cell death is a pathophysiological characteristic feature. Tryptamine produced in human gut at micro-molar concentrations reduces a number of WARS gene copies in human cells. Tryptamine-induced cell death, amyloidosis, and plaques causing damage in vasculature and microvasculature may lead to a partial liver bypassing for tryptamine transport from the gut to system. Here, the alterations in Trp-tryptamine pathway were suggested as pathogenic factors linking AD to associated diseases. A high fecal tryptamine was detected in some healthy humans (Supplemental Figure S1). Therefore, the fecal tryptamine elevation is proposed here as a possible early warning sign of tryptamine-induced cytotoxicity and neurotoxicity that is preceding AD and AD-associated diseases. The two human gut bacterial strains containing ADAS at 100% or 89% nucleotide identity were revealed in ~67 individuals out of 1246 participants from 17 human gut metagenomic studies. Both bacterial variants were present in the same groups of C&A and morbidly obese patients but not in the same individual. Bacterial sequences at ADAS 100% identity were revealed in Washington, DC; Oklahoma, USA; Denmark, and China, while at 89% identity distributed worldwide. Both cultured (89%) and uncultured (100%) bacteria are suitable for non-invasive stool testing. Our study finds new evidence that human gut bacteria play a role in AD and AD-associated diseases. Additional research needed to determine whether a role of ADAS+ bacteria is causative. In our experimental cell and animal models, human gut microbial metabolite tryptamine induces Alzheimer-like neurodegeneration. Tryptamine presents in human diet. The presence of ADAS correlates with tryptamine increase in a group of cell death-related diseases (Supplemental Table S4). Cytotoxic/neurotoxic/mitogenic tryptamine can be decontaminated and tryptamine-producing bacteria eradicated from the human body and food (www.stopalzheimerstest.com). In total, 74 BA-producing or BA-degrading strains were isolated from the human gut.[152]

Author Contributions

Conceived and designed the experiments: ELP. Analyzed the data: ELP. Wrote the first draft of the manuscript: ELP. contribution to the writing of the manuscript: ELP. Agree with manuscript results and conclusions: ELP. Exclusively developed the structure and arguments for the paper: ELP. Made critical revisions and approved final version: ELP. Author reviewed and approved the final manuscript.

Supplemental Material

Supplemental material for this article is available online.

ORCID iD

Elena L Paley https://orcid.org/0000-0002-4502-0123

REFERENCES

1. Paley EL, Merkulova-Rainon T, Faynboym A, Shestopalov VI, Aksenoff I. Geographical distribution and diversity of gut microbial NADH oxidoreductase sequence associated with Alzheimer's disease. *J Alzheimers Dis*. 2018;61:1531–1540.
2. Giau VV, Wu SY, Jamerlan A, An SSA, Kim SY, Hulme J. Gut microbiota and their neuroinflammatory implications in Alzheimer's disease. *Nutrients*. 2018;10:E1765.
3. Vogt NM, Kerby RL, Dill-McFarland KA, et al. Gut microbiome alterations in Alzheimer's disease. *Sci Rep*. 2017;7:13537.
4. Paley EL, Baranov VN, Alexandrova NM, Kisselev LL. Tryptophanyl-tRNA synthetase in cell lines resistant to tryptophan analogs. *Exp Cell Res*. 1991;195:66–78.
5. Paley EL, Perry G. Towards an integrative understanding of tRNA aminoacylation-diet-host-gut microbiome interactions in neurodegeneration. *Nutrients*. 2018;10:410.
6. Paley EL, Paley DE, Merkulova-Rainon T, Subbarayan PR. Hypoxia signature of splice forms of tryptophanyl-tRNA synthetase marks pancreatic cancer cells with distinct metastatic abilities. *Pancreas*. 2011;40:1043–1056.
7. Paley EL. Tryptamine-mediated stabilization of tryptophanyl-tRNA synthetase in human cervical carcinoma cell line. *Cancer Lett*. 1999;137:1–7.
8. Paley EL. Tryptamine-induced tryptophanyl-tRNAtrp deficiency in neurodifferentiation and neurodegeneration interplay: progenitor activation with neurite growth terminated in Alzheimer's disease neuronal vesicularization and fragmentation. *J Alzheimers Dis*. 2011;26:263–298.
9. Nemecek GM, Coughlin SR, Handley DA, Moskowitz MA. Stimulation of aortic smooth muscle cell mitogenesis by serotonin. *Proc Natl Acad Sci U S A*. 1986;83:674–678.
10. Wang F, Herrington M, Larsson J, Permert J. The relationship between diabetes and pancreatic cancer. *Mol Cancer*. 2003;2:4.
11. Jiang S, Wang Q, Huang Z, et al. Gastric bypass surgery reverses diabetic phenotypes in Bdnf-deficient mice. *Am J Pathol*. 2016;186:2117–2128.
12. Paley EL, Denisova G, Sokolova O, Posternak N, Wang X, Brownell AL. Tryptamine induces tryptophanyl-tRNA synthetase-mediated neurodegeneration with neurofibrillary tangles in human cell and mouse models. *Neuromolecular Med*. 2007;9:55–82.
13. Paley EL, Massino Yu S, Baranov VN, Alexandrova NM. Fourth International Nephrotoxicity Symposium: mechanisms of nephrotoxicity: the basis for early diagnosis, modulation of effects, and improved therapeutic management. *Ren Fail*. 1989;11:223–286.
14. Paley EL, Perry G, Sokolova O. Tryptamine induces axonopathy and mitochondriopathy mimicking neurodegenerative diseases via tryptophanyl-tRNA deficiency. *Curr Alzheimer Res*. 2013;10:987–1004.
15. Arakaki AK, Mezencev R, Bowen NJ, Huang Y, McDonald JF, Skolnick J. Identification of metabolites with anticancer properties by computational metabolomics. *Mol Cancer*. 2008;7:57
16. Herrera F, Martin V, Carrera P, et al. Tryptamine induces cell death with ultrastructural features of autophagy in neurons and glia: possible relevance for neurodegenerative disorders. *Anat Rec A Discov Mol Cell Evol Biol*. 2006;288:1026–1030.
17. Luqman A, Nega M, Nguyen MT, Ebner P, Gotz F. SadA-expressing staphylococci in the human gut show increased cell adherence and internalization. *Cell Rep*. 2018;22:535–545.
18. Maxwell DR, Gray WR, Taylor EM. Relative activity of some inhibitors of mono-amine oxidase in potentiating the action of tryptamine in vitro and in vivo. *Br J Pharmacol Chemother*. 1961;17:310–320.
19. Denckla WD, Dewey HK. Tryptamine toxicity in adrenalectomized rats; its prevention with tryptamine and hydrocortisone. *J Pharmacol Exp Ther*. 1967;158:128–134.
20. Churro C, Fernandes AS, Alverca E., et al. Effects of tryptamine on growth, ultrastructure, and oxidative stress of cyanobacteria and microalgae cultures. *Hydrobiologia*. 2010;649:195–206.
21. Fromant M, Fayat G, Laufer P, Blanquet S. Affinity chromatography of aminoacyl-tRNA syntheses on agarose-hexyl-adenosine-5'-phosphate. *Biochimie*. 1981;63:541–553.
22. Barrett OJ, Childs JL, Disney MD. Chemical microarrays to identify ligands that bind pathogenic cells. *Chembiochem*. 2006;7:1882–1885.
23. Atanassova MR, Fernandez-Otero C, Rodriguez-Alonso P, Fernandez-No IC, Garabal JI, Centeno JA. Characterization of yeasts isolated from artisanal short-ripened cows' cheeses produced in Galicia (NW Spain). *Food Microbiol*. 2016;53:172–181.
24. Gonzalez B, Vazquez J, Cullen PJ, Mas A, Beltran G, Torija MJ. Aromatic amino acid-derived compounds induce morphological changes and modulate the cell growth of wine yeast species. *Front Microbiol*. 2018;9:670.
25. Shaala LA, Youssef DT. Identification and bioactivity of compounds from the fungus Penicillium sp. CYE-87 isolated from a marine tunicate. *Mar Drugs*. 2015;13:1698–1709
26. Wust N, Rauscher-Gabernig E, Steinwider J, Bauer F, Paulsen P. Risk assessment of dietary exposure to tryptamine for the Austrian population. *Food Addit Contam Part A Chem Anal Control Expo Risk Assess*. 2017;34:404–420
27. Voigt MN, Eitenmiller RR, Koehler PE, Hamdy MK. Tyramine, histamine, and tryptamine content of cheese. *J Milk Food Technol*. 1974;37:377–381.
28. Ouellette SP, Rueden KJ, Rucks EA. Tryptophan codon-dependent transcription in chlamydia pneumoniae during gamma interferon-mediated tryptophan limitation. *Infect Immun*. 2016;84:2703–2713.
29. Sankaranarayanan K, Ozga AT, Warinner C, et al. Gut microbiome diversity among Cheyenne and Arapaho individuals from Western Oklahoma. *Curr Biol*. 2015;25:3161–3169.
30. Obregon-Tito AJ, Tito RY, Metcalf J, et al. Subsistence strategies in traditional societies distinguish gut microbiomes. *Nat Commun*. 2015;6:6505.
31. Dehaven CD, Evans AM, Dai H, Lawton KA. Organization of GC/MS and LC/MS metabolomics data into chemical libraries. *J Cheminform*. 2010;2:9.
32. Paley EL. Phosphorylation of T antigen and p53 in carcinogen-treated SV40-transformed Chinese hamster cells. *Carcinogenesis*. 1996;17:939–945.
33. Paley EL, Smelyanski L, Malinovskii V, et al. Mapping and molecular characterization of novel monoclonal antibodies to conformational epitopes on NH2 and COOH termini of mammalian tryptophanyl-tRNA synthetase reveal link of the epitopes to aggregation and Alzheimer's disease. *Mol Immunol*. 2007; 44:541–557.
34. Profenno LA, Porsteinsson AP, Faraone SV. Meta-analysis of Alzheimer's disease risk with obesity, diabetes, and related disorders. *Biol Psychiatry*. 2010;67: 505–512.
35. Yu J, Feng Q, Wong SH, et al. Metagenomic analysis of faecal microbiome as a tool towards targeted non-invasive biomarkers for colorectal cancer. *Gut*. 2017;66:70–78.
36. Heavin SB, Brennan OM, Morrissey JP, O'Byrne CP. Inhibition of Listeria monocytogenes by acetate, benzoate and sorbate: weak acid tolerance is not influenced by the glutamate decarboxylase system. *Lett Appl Microbiol*. 2009;49:179–185.
37. Lin CH, Lin CH, Chang YC, et al. Sodium benzoate, a D-amino acid oxidase inhibitor, added to clozapine for the treatment of schizophrenia: a randomized, double-blind, placebo-controlled trial. *Biol Psychiatry*. 2018;84:422–432.
38. Egashira T, Sakai K, Takayama F, Sakurai M, Yoshida S. Zinc benzoate, a contaminating environmental compound derived from polystyrene resin inhibits A-type monoamine oxidase. *Toxicol Lett*. 2003;145:161–165.
39. Sinha R, Ahn J, Sampson JN, et al. Fecal microbiota, fecal metabolome, and colorectal cancer interrelations. *PLoS ONE*. 2016;11:e0152126.
40. O'Rourke L, Clarke G, Nolan A, et al. Tryptophan metabolic profile in term and preterm breast milk: implications for health. *J Nutr Sci*. 2018;7:e13.
41. Gondalia SV, Mahon PJ, Palomboa EA, Knowlesa SR, Austina DW. Evaluation of biogenic amines in the faeces of children with and without autism by LC-MS/MS. *Int J Biotech Biochem*. 2013;9:245–255
42. Habibzadeh F, Habibzadeh P, Yadollahie M. On determining the most appropriate test cut-off value: the case of tests with continuous results. *Biochem Med (Zagreb)*. 2016;26:297–307.
43. Gevi F, Zolla L, Gabriele S, Persico AM. Urinary metabolomics of young Italian autistic children supports abnormal tryptophan and purine metabolism. *Mol Autism*. 2016;7:47
44. Wu W, Nicolazzo JA, Wen L, et al. Expression of tryptophan 2,3-dioxygenase and production of kynurenine pathway metabolites in triple transgenic mice and human Alzheimer's disease brain. *PLoS ONE*. 2013;8:e59749.
45. Trushina E, Dutta T, Persson XM, Mielke MM, Petersen RC. Identification of altered metabolic pathways in plasma and CSF in mild cognitive impairment and Alzheimer's disease using metabolomics. *PLoS ONE*. 2013;8:e63644.
46. Chyan YJ, Poeggeler B, Omar RA, et al. Potent neuroprotective properties against the Alzheimer beta-amyloid by an endogenous melatonin-related indole structure, indole-3-propionic acid. *J Biol Chem*. 1999;274: 21937–21942.
47. Davis PJ, Gustafson ME, Rosazza JP. Formation of indole-3-carboxylic acid by Chromobacterium violaceum. *J Bacteriol*. 1976;126:544–546.
48. Felix C, Salvatore MM, DellaGreca M, et al. Production of toxic metabolites by two strains of Lasiodiplodia theobromae, isolated from a coconut tree and a human patient. *Mycologia*. 2018;110:642–653.
49. Byrd DJ, Berthold HW, Trefz KF, et al. Indolic tryptophan metabolism in uraemia. *Proc Eur Dial Transplant Assoc*. 1976;12:347–354.
50. Gamir J, Pastor V, Cerezo M, Flors V. Identification of indole-3-carboxylic acid as mediator of priming against Plectosphaerella cucumerina. *Plant Physiol Biochem*. 2012;61:169–179.
51. Palleja A, Kashani A, Allin KH, et al. Roux-en-Y gastric bypass surgery of morbidly obese patients induces swift and persistent changes of the individual gut microbiota. *Genome Med*. 2016;8:67.
52. Brandacher G, Winkler C, Aigner F, et al. Bariatric surgery cannot prevent tryptophan depletion due to chronic immune activation in morbidly obese patients. *Obes Surg*. 2006;16:541–548.

53. Sarosiek K, Pappan KL, Gandhi AV, et al. Conserved metabolic changes in non-diabetic and type 2 diabetic bariatric surgery patients: global metabolomic pilot study. *J Diabetes Res*. 2016;2016:3467403.
54. Crawford C, Sepulveda MF, Elliott J, Harris PA, Bailey SR. Dietary fructan carbohydrate increases amine production in the equine large intestine: implications for pasture-associated laminitis. *J Anim Sci*. 2007;85:2949–2958.
55. Yilmaz Y, Ozdogan O. Liver disease as a risk factor for cognitive decline and dementia: an under-recognized issue. *Hepatology*. 2009;49:698.
56. Mousseau DD, Layrargues GP, Butterworth RF. Region-selective decreases in densities of [3H] binding sites in autopsied brain tissue from cirrhotic patients with hepatic encephalopathy. *J Neurochem*. 1994;62:621–625.
57. Luedde T, Kaplowitz N, Schwabe RF. Cell death and cell death responses in liver disease: mechanisms and clinical relevance. *Gastroenterology*. 2014;147:765–783.e4.
58. Babiloni C, Vecchio F, Del Percio C, et al. Resting state cortical electroencephalographic rhythms in covert hepatic encephalopathy and Alzheimer's disease. *J Alzheimers Dis*. 2013;34:707–725.
59. Balzano T, Forteza J, Molina P, et al. The cerebellum of patients with steatohepatitis shows lymphocyte infiltration, microglial activation and loss of Purkinje and granular neurons. *Sci Rep*. 2018;8:3004.
60. Karlsson FH, Fak F, Nookaew I, et al. Symptomatic atherosclerosis is associated with an altered gut metagenome. *Nat Commun*. 2012;3:1245.
61. Bedarf JR, Hildebrand F, Coelho LP, et al. Functional implications of microbial and viral gut metagenome changes in early stage L-DOPA-naive Parkinson's disease patients. *Genome Med*. 2017;9:39
62. Kumar R, Maynard CL, Eipers P, et al. Colonization potential to reconstitute a microbe community in patients detected early after fecal microbe transplant for recurrent C. Difficile. *BMC Microbiol*. 2016;16:5.
63. Vaughn BP, Vatanen T, Allegretti JR, et al. Increased intestinal microbial diversity following fecal microbiota transplant for active Crohn's disease. *Inflamm Bowel Dis*. 2016;22:2182–2190.
64. Ponnusamy K, Choi JN, Kim J, Lee SY, Lee CH. Microbial community and metabolomic comparison of irritable bowel syndrome faeces. *J Med Microbiol*. 2011;60:817–827.
65. Nikolaus S, Schulte B, Al-Massad N, et al. Increased tryptophan metabolism is associated with activity of inflammatory bowel diseases. *Gastroenterology*. 2017;153:1504–116.e2.
66. Bhattarai Y, Williams BB, Battaglioli EJ, et al. Gut microbiota-produced tryptamine activates an epithelial G-Protein-coupled receptor to increase colonic secretion. *Cell Host Microbe*. 2018;23:775–785.e5.
67. Browne HP, Forster SC, Anonye BO, et al. Culturing of "unculturable" human microbiota reveals novel taxa and extensive sporulation. *Nature*. 2016;533:543–546.
68. Raymond F, Ouameur AA, Deraspe M, et al. The initial state of the human gut microbiome determines its reshaping by antibiotics. *ISME J*. 2016;10:707–720.
69. French S, Martin K, Patterson T, Bauerle R, Miller OL Jr. Electron microscopic visualization of Trp operon expression in Salmonella typhimurium. *Proc Natl Acad Sci U S A*. 1985;82:4638–4642.
70. Reddy MV, Storer RD, Laws GM, et al. Genotoxicity of naturally occurring indole compounds: correlation between covalent DNA binding and other genotoxicity tests. *Environ Mol Mutagen*. 2002;40:1–17.
71. Sykora P, Misiak M, Wang Y, et al. DNA polymerase beta deficiency leads to neurodegeneration and exacerbates Alzheimer disease phenotypes. *Nucleic Acids Res*. 2015;43:943–959.
72. Fagerberg L, Hallstrom BM, Oksvold P, et al. Analysis of the human tissue-specific expression by genome-wide integration of transcriptomics and antibody-based proteomics. *Mol Cell Proteomics*. 2014;13:397–406.
73. Ishida T, Ueda H, Segawa K, Doi M, Inoue M. Prominent stacking interaction with aromatic amino acid by N-quarternization of nucleic acid base: X-ray crystallographic characteristics and biological implications. *Arch Biochem Biophys*. 1990;278:217–227.
74. Elias-Sonnenschein LS, Helisalmi S, Natunen T, et al. Genetic loci associated with Alzheimer's disease and cerebrospinal fluid biomarkers in a Finnish case-control cohort. *PLoS ONE*. 2013;8:e59676.
75. Burke EA, Frucht SJ, Thompson K, et al. Biallelic mutations in mitochondrial Tryptophanyl-tRNA synthetase cause levodopa-responsive infantile-onset parkinsonism. *Clin Genet*. 2017;93:712–718.
76. Serrano-Pozo A, Frosch MP, Masliah E, Hyman BT. Neuropathological alterations in Alzheimer disease. *Cold Spring Harb Perspect Med*. 2011;1:a006189.
77. Wolfgarten M, Magarey FR. Vascular fibrinoid necrosis in hypertension. *J Pathol Bacteriol*. 1959;77:597–603.
78. Kerenyi T, Jellinek H, Huttner I, Goracz G, Konyar E. Fibrinoid necrosis of the vascular wall in experimental malignant hypertension. *Acta Morphol Acad Sci Hung*. 1966;14:175–182.
79. Astrom A, Samelius U. The action of 5-hydroxytryptamine and some of its antagonists on the umbilical vessels of the human placenta. *Br J Pharmacol Chemother*. 1957;12:410–414.
80. Ginzel KH, Kottegoda SR. A study of the vascular actions of 5-hydroxytryptamine, tryptamine, adrenaline and noradrenaline. *Q J Exp Physiol Cogn Med Sci*. 1953;38:225–231.
81. Jacob J, Michaud G. [Effect of 5-hydroxytrptamine and nicotine on hypertension induced by 5-hydroxytryptamine, nicotine, tryptamine and acetaldehyde]. *Arch Int Pharmacodyn Ther*. 1962;140:92–104.
82. Anwar MA, Ford WR, Herbert AA, Broadley KJ. Signal transduction and modulating pathways in tryptamine-evoked vasopressor responses of the rat isolated perfused mesenteric bed. *Vascul Pharmacol*. 2013;58:140–149.
83. Elliott J, Berhane Y, Bailey SR. Effects of monoamines formed in the cecum of horses on equine digital blood vessels and platelets. *Am J Vet Res*. 2003;64:1124–1131.
84. Alabaster VA, Bakhle YS. Release of smooth muscle-contracting substances from isolated perfused lungs. *Eur J Pharmacol*. 1976;35:349–360.
85. Kalaria RN. The blood-brain barrier and cerebrovascular pathology in Alzheimer's disease. *Ann N Y Acad Sci*. 1999;893:113–125.
86. Ponziani FR, Zocco MA, Campanale C, et al. Portal vein thrombosis: insight into physiopathology, diagnosis, and treatment. *World J Gastroenterol*. 2010;16:143–155.
87. Rocken C, Saeger W, Linke RR. Portal amyloid: novel amyloid deposits in gastrointestinal veins? *Arch Pathol Lab Med*. 1996;120:1044–1051.
88. Gorsi U, Kalra N, Gupta P, et al. Endovascular transjugular occlusion of congenital intrahepatic portosystemic venous shunt using simultaneous fluoroscopy and transabdominal ultrasound guidance: report of 2 cases. *Curr Probl Diagn Radiol*. 2018;18:30017.
89. Papamichail M, Pizanias M, Heaton N. Congenital portosystemic venous shunt. *Eur J Pediatr*. 2018;177:285–294.
90. Meyer EP, Ulmann-Schuler A, Staufenbiel M, Krucker T. Altered morphology and 3D architecture of brain vasculature in a mouse model for Alzheimer's disease. *Proc Natl Acad Sci U S A*. 2008;105:3587–3592.
91. Desai BS, Schneider JA, Li JL, Carvey PM, Hendey B. Evidence of angiogenic vessels in Alzheimer's disease. *J Neural Transm (Vienna)*. 2009;116:587–597.
92. Vogtmann E, Hua X, Zeller G, et al. Colorectal cancer and the human gut microbiome: reproducibility with whole-genome shotgun sequencing. *PLoS ONE*. 2016;11:e0155362.
93. Ghanipour A, Jirstrom K, Ponten F, Glimelius B, Pahlman L, Birgisson H. The prognostic significance of tryptophanyl-tRNA synthetase in colorectal cancer. *Cancer Epidemiol Biomark Prev*. 2009;18:2949–2956.
94. Ogawa M, Watanabe M, Hasegawa T, Ichihara K, Yoshida K, Yanaga K. Expression of CXCR-4 and IDO in human colorectal cancer: an immunohistochemical approach. *Mol Clin Oncol*. 2017;6:701–704.
95. Beydoun MA, Beydoun HA, Gamaldo AA, et al. Nationwide inpatient prevalence, predictors, and outcomes of Alzheimer's disease among older adults in the United States, 2002-2012. *J Alzheimers Dis*. 2015;48:361–375.
96. Goedert JJ, Sampson JN, Moore SC, et al. Fecal metabolomics: assay performance and association with colorectal cancer. *Carcinogenesis*. 2014;35:2089–2096.
97. Brown DG, Rao S, Weir TL, et al. Metabolomics and metabolic pathway networks from human colorectal cancers, adjacent mucosa, and stool. *Cancer Metab*. 2016;4:11
98. Pollheimer MJ, Kornprat P, Lindtner RA, et al. Tumor necrosis is a new promising prognostic factor in colorectal cancer. *Hum Pathol*. 2010;41:1749–1757.
99. Eguchi A, Feldstein AE. Adipocyte cell death, fatty liver disease and associated metabolic disorders. *Dig Dis*. 2014;32:579–585.
100. Haase J, Weyer U, Immig K, et al. Local proliferation of macrophages in adipose tissue during obesity-induced inflammation. *Diabetologia*. 2014;57:562–571.
101. Moh C, Kubiak JZ, Bajic VP, Zhu X, Smith MA, Lee HG. Cell cycle deregulation in the neurons of Alzheimer's disease. *Results Probl Cell Differ*. 2011;53:565–576.
102. Driver JA, Beiser A, Au R, et al. Inverse association between cancer and Alzheimer's disease: results from the Framingham Heart Study. *BMJ*. 2012;344:e1442.
103. Caini S, Bagnoli S, Palli D, et al. Total and cancer mortality in a cohort of ulcerative colitis and Crohn's disease patients: the Florence inflammatory bowel disease study, 1978-2010. *Dig Liver Dis*. 2016;48:1162–1167.
104. Holmberg FEO, Pedersen J, Jorgensen P, Soendergaard C, Jensen KB, Nielsen OH. Intestinal barrier integrity and inflammatory bowel disease: stem cell-based approaches to regenerate the barrier. *J Tissue Eng Regen Med*. 2018;12:923–935.
105. Li Y, Wang D, Zeng C, Liu Y, Huang G, Mei Z. Salivary metabolomics profile of patients with recurrent aphthous ulcer as revealed by liquid chromatography-tandem mass spectrometry. *J Int Med Res*. 2018;46:1052–1062.
106. Lankarani KB, Sivandzadeh GR, Hassanpour S. Oral manifestation in inflammatory bowel disease: a review. *World J Gastroenterol*. 2013;19:8571–8579.
107. Dyson JK, Rutter MD. Colorectal cancer in inflammatory bowel disease: what is the real magnitude of the risk? *World J Gastroenterol*. 2012;18:3839–3848.
108. van Langenberg DR, Yelland GW, Robinson SR, Gibson PR. Cognitive impairment in Crohn's disease is associated with systemic inflammation, symptom burden and sleep disturbance. *United European Gastroenterol J*. 2017;5:579–587.

109. Wen C, Zheng Z, Shao T, et al. Quantitative metagenomics reveals unique gut microbiome biomarkers in ankylosing spondylitis. *Genome Biol*. 2017;18:142.
110. Backhed F, Roswall J, Peng Y, et al. Dynamics and stabilization of the human gut microbiome during the first year of life. *Cell Host Microbe*. 2015;17:690–703.
111. Gibson MK, Wang B, Ahmadi S, et al. Developmental dynamics of the preterm infant gut microbiota and antibiotic resistome. *Nat Microbiol*. 2016;1:16024.
112. Barry KA, Wojcicki BJ, Middelbos IS, et al. Dietary cellulose, fructooligosaccharides, and pectin modify fecal protein catabolites and microbial populations in adult cats. *J Anim Sci*. 2010;88:2978–2987.
113. Saraf MK, Piccolo BD, Bowlin AK, et al. Formula diet driven microbiota shifts tryptophan metabolism from serotonin to tryptamine in neonatal porcine colon. *Microbiome*. 2017;5:77.
114. Chow J, Panasevich MR, Alexander D, et al. Fecal metabolomics of healthy breast-fed versus formula-fed infants before and during in vitro batch culture fermentation. *J Proteome Res*. 2014;13:2534–2542.
115. Candia OA, Alvarez LJ, Lanzetta PA, Cook P. Tryptamine in the vertebrate lens. *Biochim Biophys Acta*. 1983;762:232–240.
116. Niyadurupola N, Astbury N. Endophthalmitis: controlling infection before and after cataract surgery. *Community Eye Health*. 2008;21:9–10.
117. Osnes-Ringen O, Berg KH, Moe MC, Zetterstrom C, Roger M, Nicolaissen B. Cell death pattern in lens epithelium of cataract patients. *Acta Ophthalmol*. 2016;94:514–520.
118. Joo CK, Lee EH, Kim JC, et al. Degeneration and transdifferentiation of human lens epithelial cells in nuclear and anterior polar cataracts. *J Cataract Refract Surg*. 1999;25:652–658.
119. Lai SW, Lin CL, Liao KF. Cataract may be a non-memory feature of Alzheimer's disease in older people. *Eur J Epidemiol*. 2014;29:405–409.
120. Swanson KS, Grieshop CM, Flickinger EA, et al. Fructooligosaccharides and Lactobacillus acidophilus modify bowel function and protein catabolites excreted by healthy humans. *J Nutr*. 2002;132:3042–3050.
121. Vasa RA, Anderson C, Marvin AR, et al. Mood disorders in mothers of children on the autism spectrum are associated with higher functioning autism. *Autism Res Treat*. 2012;2012:435646.
122. Uppal N, Wicinski B, Buxbaum JD, Heinsen H, Schmitz C, Hof PR. Neuropathology of the anterior midcingulate cortex in young children with autism. *J Neuropathol Exp Neurol*. 2014;73:891–902.
123. Lee M, Krishnamurthy J, Susi A, et al. Association of autism spectrum disorders and inflammatory bowel disease. *J Autism Dev Disord*. 2018;48:1523–1529.
124. Radulovacki P, Djuricic-Nedelson M, Chen EH, Radulovacki M. Human tryptamine metabolism decreases during night sleep. *Brain Res Bull*. 1983;10:43–45.
125. Luan H, Liu LF, Meng N, et al. LC-MS-based urinary metabolite signatures in idiopathic Parkinson's disease. *J Proteome Res*. 2015;14:467–478.
126. D'Andrea G, Bussone G, Di Fiore P, et al. Pathogenesis of chronic cluster headache and bouts: role of tryptamine, arginine metabolism and alpha1-agonists. *Neurol Sci*. 2017;38:37–43.
127. Valfre W, Rainero I, Bergui M, Pinessi L. Voxel-based morphometry reveals gray matter abnormalities in migraine. *Headache*. 2008;48:109–117.
128. Benemei S, Nicoletti P, Geppetti P, Bonciani M. Cataract in chronic cluster headache: two case reports and review of the literature. *J Headache Pain*. 2008;9:401–403.
129. Mijajlovic MD, Aleksic VM, Covickovic Sternic NM. Cluster headache as a first manifestation of multiple sclerosis: case report and literature review. *Neuropsychiatr Dis Treat*. 2014;10:2269–2274.
130. Tanimukai H, Ginther R, Spaide J, Bueno JR, Himwich HE. Detection of psychotomimetic N-dimethylated indoleamines in the urine of four schizophrenic patients. *Br J Psychiatry*. 1970;117:421–430.
131. Sullivan JP, McDonnell L, Hardiman OM, Farrell MA, Phillips JP, Tipton KF. The oxidation of tryptamine by the two forms of monoamine oxidase in human tissues. *Biochem Pharmacol*. 1986;35:3255–3260.
132. Saura J, Nadal E, van den Berg B, Vila M, Bombi JA, Mahy N. Localization of monoamine oxidases in human peripheral tissues. *Life Sci*. 1996;59:1341–1349.
133. Rybaczyk LA, Bashaw MJ, Pathak DR, Huang K. An indicator of cancer: down-regulation of monoamine oxidase-A in multiple organs and species. *BMC Genomics*. 2008;9:134.
134. Eo J, Lee HE, Nam GH, et al. Association of DNA methylation and monoamine oxidase A gene expression in the brains of different dog breeds. *Gene*. 2016;580:177–182.
135. Mousseau DD. Tryptamine: a metabolite of tryptophan implicated in various neuropsychiatric disorders. *Metab Brain Dis*. 1993;8:1–44.
136. Gahr M, Schonfeldt-Lecuona C, Kolle MA, Freudenmann RW. Intoxications with the monoamine oxidase inhibitor tranylcypromine: an analysis of fatal and non-fatal events. *Eur Neuropsychopharmacol*. 2013;23:1364–1372.
137. Kennedy D, Webster WS, Hill M, Ritchie HE. Abnormal pregnancy outcome associated with high-dose maternal tranylcypromine therapy: case report and literature review. *Reprod Toxicol*. 2017;69:146–149.
138. White N, Litovitz T, Clancy C. Suicidal antidepressant overdoses: a comparative analysis by antidepressant type. *J Med Toxicol*. 2008;4:238–250.
139. Green H, Sawyer JL. Correlation of tryptamine-induced convulsions in rats with brain tryptamine concentration. *Proc Soc Exp Biol Med*. 1960;104:153–155.
140. Baker GB, Coutts RT, McKenna KF, Sherry-McKenna RL. Insights into the mechanisms of action of the MAO inhibitors phenelzine and tranylcypromine: a review. *J Psychiatry Neurosci*. 1992;17:206–214.
141. Bieck PR, Antonin KH. Monoamine oxidase inhibition by tranylcypromine: assessment in human volunteers. *Eur J Clin Pharmacol*. 1982;22:301–308.
142. Bieck PR, Firkusny L, Schick C, et al. Monoamine oxidase inhibition by phenelzine and brofaromine in healthy volunteers. *Clin Pharmacol Ther*. 1989;45:260–269.
143. Callaway JC, Airaksinen MM, Salmela KS, Salaspuro M. Formation of tetrahydroharman (1-methyl-1,2,3,4-tetrahydro-beta-carboline) by Helicobacter pylori in the presence of ethanol and tryptamine. *Life Sci*. 1996;58:1817–1821.
144. Susilo R, Damm H, Rommelspacher H, Hofle G. Biotransformation of 1-methyl-1,2,3,4-tetrahydro-beta-carboline-1-carboxylic acid to harmalan, tetrahydroharman and harman in rats. *Neurosci Lett*. 1987;81:325–330.
145. Santillo MF, Liu Y, Ferguson M, Vohra SN, Wiesenfeld PL. Inhibition of monoamine oxidase (MAO) by beta-carbolines and their interactions in live neuronal (PC12) and liver (HuH-7 and MH1C1) cells. *Toxicol in Vitro*. 2014;28:403–410.
146. Liu S, Liang S, Liu H, et al. Metabolite profiling of feces and serum in hemodialysis patients and the effect of medicinal charcoal tablets. *Kidney Blood Press Res*. 2018;43:755–767.
147. Brito JS, Borges NA, Esgalhado M, Magliano DC, Soulage CO, Mafra D. Aryl hydrocarbon receptor activation in chronic kidney disease: role of uremic toxins. *Nephron*. 2017;137:1–7.
148. Naka K, Watarai S, Tana, et al. Adsorption effect of activated charcoal on enterohemorrhagic Escherichia coli. *J Vet Med Sci*. 2001;63:281–285.
149. Hamdani N, Boukouaci W, Hallouche MR, et al. Resolution of a manic episode treated with activated charcoal: evidence for a brain-gut axis in bipolar disorder. *Aust N Z J Psychiatry*. 2015;49:1221–1223.
150. Skogvall S, Erjefalt JS, Olin AI, Ankerst J, Bjermer L. Oral iodinated activated charcoal improves lung function in patients with COPD. *Respir Med*. 2014;108:905–909.
151. Pfab R, Schmoll S, Dostal G, Stenzel J, Hapfelmeier A, Eyer F. Single dose activated charcoal for gut decontamination: application by medical non-professionals -a prospective study on availability and practicability. *Toxicol Rep*. 2017;4:49–54.
152. Pugin B, Barcik W, Westermann P, et al. A wide diversity of bacteria from the human gut produces and degrades biogenic amines. *Microb Ecol Health Dis*. 2017;28:1353881.